APPENDIX - FOR ONLINE PUBLICATION

Why Does the Fed Move Markets so Much? A Model of Monetary Policy and Time-Varying Risk Aversion

Carolin Pflueger and Gianluca Rinaldi[1]

September 2020

[1]Pflueger: University of Chicago, Harris School of Public Policy, NBER, and CEPR. Email cpflueger@uchicago.edu. Rinaldi: Harvard University. Email rinaldi@g.harvard.edu.

A Loglinear habit dynamics around steady state

This section derives the loglinear dynamics of the habit stock using a first order approximation around the steady state $S_t = \bar{S}$. We write log habit h_t as a distributed lag of moments of consumption, the habit shock $\varepsilon_{s,t}$, and the output gap, which also equals the deviation of log consumption from the frictionless level. This loglinear expansion therefore implies that we can broadly view habit as a function of (lags of) consumption moments, and the shock $\varepsilon_{s,t}$, which for this reason we refer to as a "habit shock".

In the paper, we model how habit adjusts to consumption implicitly by modeling the evolution of the log surplus consumption ratio. In order to solve for log habit we need an approximate relation between log habit, log consumption, and the log surplus consumption ratio. Defining $\hat{s}_t = s_t - \bar{s}$, we develop a first-order Taylor expansion of $\hat{s}_t$ in terms of $c_t - h_t$. We take the first derivative of $\hat{s}_t$ with respect to $c_t - h_t$:

$$\frac{d\hat{s}_t}{d(c_t - h_t)} = \frac{d}{d(c_t - h_t)}\left(\log\left(\frac{1 - exp(-(c_t - h_t))}{\bar{S}}\right)\right), \tag{A1}$$

$$= \frac{\bar{S}}{1 - exp(-(c_t - h_t))}\frac{exp(-(c_t - h_t))}{\bar{S}}, \tag{A2}$$

$$= -\left(1 - \frac{1}{S_t}\right), \tag{A3}$$

so at the steady state this first derivative equals:

$$\left.\frac{d\hat{s}_t}{d(c_t - h_t)}\right|_{S_t = \bar{S}} = -\left(1 - \frac{1}{\bar{S}}\right). \tag{A4}$$

The first order Taylor expansion for $\hat{s}_t$ in terms of $c_t - h_t$ around the steady-state therefore equals (up to constant):

$$\hat{s}_t \approx \left(1 - \frac{1}{\bar{S}}\right)(h_t - c_t), \tag{A5}$$

or

$$h_t \approx c_t + \frac{\hat{s}_t}{1 - \frac{1}{\bar{S}}}. \tag{A6}$$

The relation (A6) is approximate rather than exact because we ignore second- and higher-order terms in $(c_t - h_t)$. Further approximating $\lambda(s_t) \approx \lambda(\bar{s}) = \frac{1}{\bar{S}} - 1$, the approximate dynamics for $\hat{s}_t$ near the steady state are given by:

$$\hat{s}_{t+1} \approx \theta_0 \hat{s}_t + \theta_1 x_t + \theta_2 x_{t-1} + \varepsilon_{s,t} + \left(\frac{1}{\bar{S}} - 1\right)\varepsilon_{c,t+1}. \tag{A7}$$

Combining (A6) with (A7) gives the approximate dynamics for log habit:

$$\begin{aligned} h_{t+1} &\approx c_{t+1} + \frac{1}{1-\frac{1}{\bar{S}}}\hat{s}_{t+1}, && \text{(A8)} \\ &\approx c_{t+1} + \frac{1}{1-\frac{1}{\bar{S}}}\left(\theta_0 \hat{s}_t + \theta_1 x_t + \theta_2 x_{t-1} + \varepsilon_{s,t} + \left(\frac{1}{\bar{S}} - 1\right)\varepsilon_{c,t+1}\right), && \text{(A9)} \\ &\approx c_{t+1} - \varepsilon_{c,t+1} + \theta_0 (h_t - c_t) - \frac{\theta_1}{\frac{1}{\bar{S}}-1}x_t - \frac{\theta_2}{\frac{1}{\bar{S}}-1}x_{t-1} - \frac{1}{\frac{1}{\bar{S}}-1}\varepsilon_{s,t}, && \text{(A10)} \\ &\approx \theta_0 h_t + (1-\theta_0)c_t + E_t\Delta c_{t+1} - \frac{\theta_1 x_t + \theta_2 x_{t-1}}{\frac{1}{\bar{S}}-1} - \frac{1}{\frac{1}{\bar{S}}-1}\varepsilon_{s,t}, && \text{(A11)} \end{aligned}$$

where we use $\Delta c_{t+1} = c_{t+1} - c_t$ to denote the change in log consumption from time t to time $t+1$. We now iterate (A11) to obtain:

$$\begin{aligned} h_{t+1} &\approx \sum_{j=0}^{\infty}\theta_0^j \left((1-\theta_0)c_{t-j} + E_{t-j}\Delta c_{t-j+1} - \frac{1}{\frac{1}{\bar{S}}-1}\varepsilon_{s,t-j} - \frac{\theta_1 x_{t-j} + \theta_2 x_{t-j-1}}{\frac{1}{\bar{S}}-1}\right), && \text{(A12)} \\ &\approx (1-\theta_0)\sum_{j=0}^{\infty}\theta_0^j c_{t-j} + \sum_{j=0}^{\infty}\theta_0^j E_{t-j}\Delta c_{t-j+1} - \frac{1}{\frac{1}{\bar{S}}-1}\sum_{j=0}^{\infty}\theta_0^j \varepsilon_{s,t-j} - \frac{\theta_1}{\frac{1}{\bar{S}}-1}x_t && \text{(A13)} \\ &\quad - \frac{\theta_0\theta_1 + \theta_2}{\frac{1}{\bar{S}}-1}\sum_{j=0}^{\infty}\theta_0^j x_{t-j-1}. && \text{(A14)} \end{aligned}$$

The expansion (A14) shows that approximate log habit depends on lagged moments of consumption, the output gap, and the habit shock. The resource constraint implies that output equals consumption, so the output gap equals the deviation of log consumption relative to a frictionless level.

In order to understand the compounded dependence of habit on the first and second lags of consumption, we substitute in for x_t from equation (25) in the main paper:

$$\begin{aligned} h_{t+1} &\approx (1-\theta_0)\sum_{j=0}^{\infty}\theta_0^j c_{t-j} + \sum_{j=0}^{\infty}\theta_0^j E_{t-j}\Delta c_{t-j+1} - \frac{1}{\frac{1}{\bar{S}}-1}\sum_{j=0}^{\infty}\theta_0^j \varepsilon_{s,t-j} && \text{(A15)} \\ &\quad - \frac{\theta_1}{\frac{1}{\bar{S}}-1}\left(c_t - (1-\phi)\sum_{i=0}^{\infty}\phi^i c_{t-1-i} - \sum_{i=0}^{\infty}\phi^i \Delta a_{t-i}\right) && \text{(A16)} \\ &\quad - \frac{\theta_0\theta_1 + \theta_2}{\frac{1}{\bar{S}}-1}\sum_{j=0}^{\infty}\theta_0^j\left(c_{t-j-1} - (1-\phi)\sum_{i=0}^{\infty}\phi^i c_{t-j-2-i} - \sum_{i=0}^{\infty}\phi^i \Delta a_{t-i-1}\right). && \text{(A17)} \end{aligned}$$

The Campbell and Cochrane (1999) case corresponds to $\theta_1 = \theta_2 = 0$ and constant expected consumption growth. In that case, expression (A17) shows that log habit is approximately an exponentially-weighted moving average of lagged log consumption with exponential parameter θ_0.

Our estimated model has $\theta_1 < 0$ and $\theta_2 > 0$, which allows us to generate hump-shaped output responses to monetary policy shocks that have been documented in macroeconomic data. Because $\frac{1}{\frac{1}{\bar{S}}-1} > 0$ and $1-\phi$ is close to zero, a negative value for θ_1 raises the sensitivity of habit to the first two lags of consumption, while a positive value for θ_2 lowers the sensitivity of habit with respect to the second lag of consumption. Our model uses $-\theta_1 > 0$, and $\theta_1(1-\phi) - (\theta_0\theta_1 + \theta_2) = 0$ (which is the condition ensuring that the forward- and backward-looking coefficients in the log-linear macro Euler equation sum to one). Equation (A17) then implies that habit loads more on the first lag of consumption than in the Campbell-Cochrane case, but the loading onto the second consumption lag is unchanged.

B Proof of Phillips Curve

The derivation of the log-linearized Phillips curve is tedious, but almost all the steps in our derivation are standard. Our asset pricing habit preferences potentially enter in two places. This section shows that the log-linearized Phillips curve is invariant to both of these channels for the following two reasons:

1. Firms' real marginal cost depends on the real wage, which depends on preferences. The log-linearized Phillips curve is invariant to this channel, because we separate the intertemporal consumption-savings decision and the intratemporal labor-leisure choice as in Greenwood, Hercowitz, and Huffman (1988). We therefore obtain a standard functional form for log-linearized real marginal cost that does not depend on habit or surplus consumption.

2. The SDF enters into firms' first-order condition for the optimal price-setting decision. The log-linearized Phillips curve is invariant to this channel, because up to first-order our SDF is standard and second-order terms drop out of the log-linearized first-order condition, leading to a standard log-linearized Phillips curve.

We log linearize inflation around its random walk component v_t^* and output and labor around the steady-state with $\bar{Y}_t = A_t \bar{L}^{1-\tau}$ and $\bar{L}$ the labor supply consistent with steady-state markups when prices are flexible. We use bars to denote steady-state values and hats to denote log deviations from this steady-state. We use lower-case letters to denote logs.

B.1 Marginal Cost of Production and Steady-State

The New Keynesian Phillips curve links inflation to the marginal cost of production. By linking the marginal cost of production to the output gap, one then obtains a relationship between inflation and output. It is therefore important to check that our asset pricing preferences give rise to a standard log-linearized expression for the *real marginal cost* of producing another unit of output. In this section, we show that log deviation of marginal cost from steady-state takes the form:

$$\hat{mc}_{i,t} = a_0 \hat{y}_t - a_1 \left(p_{i,t} - p_t\right), \tag{A18}$$

i.e. it increases in the log deviation of output from the steady state, and decreases in the log own-firm price deviation from the log aggregate price level where both a_0 and a_1 are positive constants.

The labor-leisure trade-off implies that the real wage paid by firms producing good i equals:

$$W_{i,t} = \left(\frac{dU}{dC_t}\right) / \left(\frac{dU}{dL_{i,t}}\right) = A_t \left(1 - L_{i,t}\right)^{-\chi}. \tag{A19}$$

The total cost of producing a quantity $Y_{i,t}$ of good i equals:

$$Cost(Y_{i,t}) = W_{i,t} \left(\frac{Y_{i,t}}{A_t}\right)^{1/(1-\tau)} \tag{A20}$$

Taking the derivative with respect to $Y_{i,t}$ gives the marginal cost of supplying good i:

$$MC(Y_{i,t}) = \frac{1}{1-\tau} \frac{W_{i,t}}{A_t} \left(\frac{Y_{i,t}}{A_t}\right)^{\frac{\tau}{1-\tau}}, \tag{A21}$$

$$= \frac{1}{1-\tau} \left(1 - \left(\frac{Y_{i,t}}{A_t}\right)^{1/(1-\tau)}\right)^{-\chi} \left(\frac{Y_{i,t}}{A_t}\right)^{\frac{\tau}{1-\tau}}. \tag{A22}$$

Note that here we have assumed that the producer is a wage taker following Woodford (2003, p.148). We define the steady-state labor supply $\bar{L}$ to be the amount of labor supplied if markups are equal to the steady-state value $\bar{\mu} = \frac{\theta}{1-\theta}$, and all firms charge the same price. From (A22), we see that $\bar{L}$ must be the solution to

$$\bar{\mu}^{-1} = \frac{1}{1-\tau} \left(1 - \bar{L}\right)^{-\chi} \bar{L}^{\frac{\tau}{1-\tau}}. \tag{A23}$$

We log-linearize around the steady-state output:

$$\bar{Y}_t = A_t \bar{L}^{1-\tau}. \tag{A24}$$

Log-linearizing the real wage around the flexible-wage steady-state gives:

$$\hat{w}_{i,t} = \chi \frac{\bar{L}}{1-\bar{L}} \hat{l}_{i,t}, \tag{A25}$$

$$= \eta \hat{l}_{i,t}, \tag{A26}$$

where $\eta \equiv \chi \frac{\bar{L}}{1-\bar{L}}$ is the inverse of the steady-state Frisch elasticity of labor supply.

The elasticity of real marginal cost with respect to own-firm output near the steady-state equals:

$$\frac{dMC_{i,t}}{dY_{i,t}} \frac{Y_{i,t}}{MC_{i,t}} = \frac{\tau}{1-\tau} + \frac{\eta}{1-\tau}, \tag{A27}$$

$$\equiv \omega. \tag{A28}$$

Using θ to denote the steady-state value of θ_t, we then approximate firm i's deviation of marginal cost from $\bar{\mu}^{-1}$ log-linearly:

$$\widehat{mc}_{i,t} = \log\left(MC_{i,t}\right) - \log\left(\bar{\mu}^{-1}\right),$$
$$= \omega \hat{y}_{i,t}, \tag{A29}$$
$$= \omega \hat{y}_t - \omega\theta(p_{i,t} - p_t), \tag{A30}$$

In the last step, we have used the demand function (15), log-linearized around the steady-state elasticity of substitution θ, to substitute $\hat{y}_{i,t} - \hat{y}_t = \theta\left(p_{i,t} - p_t\right)$. We hence obtain the functional form (A18) with $a_0 = \omega$ and $a_1 = \omega\theta$.

We can compare (A30) to the log real marginal cost obtained with standard preferences (e.g. Woodford, 2003), where the real wage is given by

$$W_t = \frac{L_{i,t}^{\eta}}{C_t^{-\gamma}}, \tag{A31}$$

where η is the inverse of the Frisch elasticity of labor supply and γ is risk aversion. This expression is log-linearized to

$$\hat{w}_{i,t} = \gamma \hat{y}_t + \eta \hat{l}_{i,t}. \tag{A32}$$

If instead, the log-linearized real wage took the form (A32), we would obtain the following log-linearized expression for the real marginal cost:

$$\widehat{mc}_{i,t} = \left(\omega + \gamma\right)\hat{y}_t - \omega\theta(p_{i,t} - p_t), \tag{A33}$$

i.e. $a_0 = \omega + \gamma$ and $a_1 = \omega\theta$. Comparing expressions (A30) and (A33) shows that the log-linearized real wage in our model takes the same functional form as under standard preferences, which is why the log-linearized Phillips curve will also take the same form.

B.2 Discount Factor for Phillips Curve

We now derive the first-order approximation of the stochastic discount factor, which is needed for the derivation of the log-linearized Phillips curve. We show that because the first-order approximation of our stochastic discount factor is standard, our asset pricing preferences do not affect the log-linearized Phillips curve. In the steady-state, log consumption grows at rate g and s_t is constant at $\bar{s}$. The steady-state SDF for discounting time $t + j$ real cash flows at time t takes the standard form:

$$\bar{M}_{t,t+j} = \beta^j exp(-\gamma g j). \tag{A34}$$

We denote log deviation of the SDF from this steady-state:

$$\hat{m}_{t,t+j} = \log\left(M_{t,t+j}/\bar{M}_{t,t+j}\right). \tag{A35}$$

We will see that $\hat{m}_{t,t+j}$ drops out of the log-linearized price-setting first-order condition, which is why we can apply all the standard tools for deriving the log-linearized Phillips curve.

B.3 Price Level Law of Motion

The price level law of motion is standard. Because we have a unit root in inflation, we are careful to follow Cogley and Sbordone (2008) in log-linearizing inflation around its random-walk trend v_t^*. Log deviations in inflation from steady-state are defined as

$$\hat{\pi}_t \;=\; \pi_t - v_t^* \tag{A36}$$

and we log-linearize around $\hat{\pi}_t = 0$.

Since the probability of being able to adjust the price-level is independent and equal across firms, each firm that has the chance to re-set its price at time t chooses the same price $\tilde{P}_t$. The law of motion for the price level is

$$P_t^{-(\theta_t-1)} \;=\; \alpha\left(P_{t-1}\frac{P_{t-1}}{P_{t-2}}\right)^{-(\theta_t-1)} + (1-\alpha)\tilde{P}_t^{-(\theta_t-1)}. \tag{A37}$$

Dividing (A37) by $P_t^{-(\theta_t-1)}$ gives

$$1 \;=\; \alpha exp\left((\theta_t-1)\left(\hat{\pi}_t - \hat{\pi}_{t-1} + v_{LT,t}\right)\right) + (1-\alpha)\left(\frac{\tilde{P}_t}{P_t}\right)^{-(\theta_t-1)}. \tag{A38}$$

Using $\tilde{p}_t$ to denote log deviations of $\frac{\tilde{P}_t}{P}$ from one, the log-linearized law of motion becomes:

$$\tilde{p}_t \;=\; \frac{\alpha}{1-\alpha}\left(\hat{\pi}_t - \hat{\pi}_{t-1} + v_{LT,t}\right). \tag{A39}$$

B.4 Price-Setting First-Order Condition

The firm's first-order condition for optimal price-setting is standard and follows Walsh (2017) while adding markup shocks and price indexing as in Cogley and Sbordone (2008) and Smets and Wouters (2007). A firm that re-sets its price at time t and does not get to re-set again during the next j periods indexes its price to the aggregate price increase from time $t-1$ to $t-1+j$ as in Smets and Wouters (2007). This means that such a firm has time $t+j$ price:

$$\tilde{P}_t\left(P_{t-1+j}/P_{t-1}\right). \tag{A40}$$

A firm that has the opportunity to re-set prices at time t chooses $\tilde{P}_t$ to maximize expected discounted profits conditional on the price still being in place:

$$\underset{\tilde{P}_t}{max} E_t \sum_{j=0}^{\infty} \alpha^j M_{t,t+j} Y_{t+j}\left(\left(\frac{\tilde{P}_t}{P_t}\frac{P_{t-1+j}/P_{t-1}}{P_{t+j}/P_t}\right)^{1-\theta_{t+j}} - \frac{Cost\left(Y_{i,t+j}\right)}{Y_{t+j}}\right) \tag{A41}$$

the first-order condition:

$$\begin{aligned} & \frac{\tilde{P}_t}{P_t} E_t \sum_{j=0}^{\infty} \alpha^j M_{t,t+j} Y_{t+j} (\theta_{t+j} - 1) \left(\frac{P_{t-1+j}/P_{t-1}}{P_{t+j}/P_t} \right)^{1-\theta_{t+j}} \\ = \; & E_t \sum_{j=0}^{\infty} \alpha^j M_{t,t+j} Y_{t+j} \theta_{t+j} \left(\frac{P_{t-1+j}/P_{t-1}}{P_{t+j}/P_t} \right)^{-\theta_{t+j}} MC_{i,t+j}. \end{aligned} \tag{A42}$$

B.5 Log-Linearization

We now log-linearize the first-order condition (A42) following the steps outlined in Walsh (2017), Chapter 8.7. In the flexible-price equilibrium with θ_t at its steady-state value θ, all firms charge the same price so $\overline{MC} = \bar{\mu}^{-1} = \frac{\theta-1}{\theta}$. Denoting the log of steady-state output by $\bar{y}_t \equiv \log \bar{Y}_t$ we have that

$$\bar{y}_{t+1} - \bar{y}_t = n_{t+1} - n_t + \Delta a_{t+1}, \tag{A43}$$

$$= \nu + (1-\phi)(1-\tau) l_t + \Delta a_{t+1}, \tag{A44}$$

$$= g + (1-\phi)\hat{y}_t + \Delta a_{t+1}, \tag{A45}$$

where the relationship between the steady-state growth rate g, ν, and ϕ is given by

$$g = \nu + (1-\phi)(1-\tau)\bar{l}. \tag{A46}$$

To save on notation, we define:

$$\beta_g = \beta exp(-(\gamma-1)g) \tag{A47}$$

and

$$\tilde{p}_t = \log\left(\tilde{P}_t / P_t\right). \tag{A48}$$

The log-linear expansion for the left-hand-side of (A42) conditional on $\bar{Y}_t$ becomes:

$$\begin{aligned} & (1+\tilde{p}_t)\, E_t \sum_{j=0}^{\infty} \Big[(\beta_g \alpha)^j\, \bar{Y}_t (1+\hat{y}_{t+j})(1+(\bar{y}_{t+j} - \bar{y}_t - g))\,(1+\hat{m}_{t,t+j}) \Big(\theta(1+\hat{\theta}_{t+j}) - 1\Big) \times \\ & \Big(1 + (1-\theta(1+\hat{\theta}_{t+j}))\Big(\hat{\pi}_t - \hat{\pi}_{t+j} + (v^{LT}_{t+1} + ... + v^{LT}_{t+j})\Big)\Big)\Big]. \end{aligned} \tag{A49}$$

Dropping second-order terms and collecting terms that are independent of j gives

$$\begin{aligned} & \frac{\bar{Y}_t(\theta-1)}{1-\beta_g\alpha} + \frac{\bar{Y}_t \tilde{p}_t (\theta-1)}{1-\beta_g\alpha} \\ & + \bar{Y}_t(\theta-1) E_t \sum_{j=0}^{\infty} (\beta_g\alpha)^j \Big(\hat{y}_{t+j} + (\bar{y}_{t+j} - \bar{y}_t - g) + \hat{m}_{t,t+j} + \bar{\mu}\hat{\theta}_{t+j} + (1-\theta)\,(\hat{\pi}_t - \hat{\pi}_{t+j})\Big). \end{aligned} \tag{A50}$$

Next, we approximate the right-hand-side of (A42) log-linearly. This gives

$$E_t \sum_{j=0}^{\infty} \Big[(\beta_g \alpha)^j \, \bar{Y}_t (1 + \hat{y}_{t+j})(1 + (\bar{y}_{t+j} - \bar{y}_t - g)) \, (1 + \hat{m}_{t,t+j}) \, \theta (1 + \hat{\theta}_{t+j}) \times$$
$$\left(1 - \theta(1 + \hat{\theta}_{t+j}) \left(\hat{\pi}_t - \hat{\pi}_{t+j} + (v_{t+1}^{LT} + ... + v_{t+j}^{LT})\right)\right) \overline{MC}(1 + \widehat{mc}_{t+j}) \Big] . \qquad \text{(A51)}$$

Next, we use $\theta \overline{MC} = \theta - 1$, note that $E_t v_{t+k}^{LT} = 0$ for $k > 0$, substitute in (A30), and drop second-order terms:

$$\frac{\bar{Y}_t(\theta - 1)}{1 - \beta_g \alpha} + \bar{Y}_t(\theta - 1) E_t \sum_{j=0}^{\infty} (\beta_g \alpha)^j \left(\hat{y}_{t+j} + (\bar{y}_{t+j} - \bar{y}_t - g) + \hat{m}_{t,t+j} + \hat{\theta}_{t+j} \right)$$
$$+ \bar{Y}_t(\theta - 1) E_t \sum_{j=0}^{\infty} (\beta_g \alpha)^j \left(-\theta \left(\hat{\pi}_t - \hat{\pi}_{t+j} \right) + \widehat{mc}_{t+j} \right) , \qquad \text{(A52)}$$
$$= \frac{\bar{Y}_t(\theta - 1)}{1 - \beta_g \alpha} + \bar{Y}_t(\theta - 1) E_t \sum_{j=0}^{\infty} (\beta_g \alpha)^j \left(\hat{y}_{t+j} + (\bar{y}_{t+j} - \bar{y}_t - g) + \hat{m}_{t,t+j} + \hat{\theta}_{t+j} \right)$$
$$+ \bar{Y}_t(\theta - 1) E_t \sum_{j=0}^{\infty} (\beta_g \alpha)^j \left(-\theta \left(\hat{\pi}_t - \hat{\pi}_{t+j} \right) + a_0 \hat{y}_{t+j} \right)$$
$$- a_1 \left(\frac{\bar{Y}_t(\theta - 1)\tilde{p}_t}{1 - \beta_g \alpha} + \bar{Y}_t(\theta - 1) E_t \sum_{j=0}^{\infty} (\beta_g \alpha)^j \left(\hat{\pi}_t - \hat{\pi}_{t+j} \right) \right) . \qquad \text{(A53)}$$

Equating (A50) and (A53), cancelling common terms, and dividing by $\bar{Y}_t(\theta - 1)$ gives

$$(1 + a_1) \left(\frac{\tilde{p}_t}{1 - \beta_g \alpha} + \frac{\hat{\pi}_t}{1 - \beta_g \alpha} - E_t \sum_{j=0}^{\infty} (\beta_g \alpha)^j \, \hat{\pi}_{t+j} \right)$$
$$= E_t \sum_{j=0}^{\infty} (\beta_g \alpha)^j \left(a_0 \hat{y}_{t+j} + \hat{\mu}_{t+j} \right) , \qquad \text{(A54)}$$

where the log deviation of the markup from steady-state is given by

$$\hat{\mu}_{t+j} = \frac{d\mu_{t+j}}{d\theta_{t+j}} \frac{\mu_{t+j}}{\theta_{t+j}} \hat{\theta}_{t+j} = \frac{1}{\theta - 1} \hat{\theta}_{t+j} = (1 - \bar{\mu}) \, \hat{\theta}_{t+j}. \qquad \text{(A55)}$$

Note in particular that $\hat{m}_{t,t+j}$ drops out of (A54). Because this is the main place where we differ from the standard New Keynesian model, this makes clear that our asset pricing preferences drop out of the log-linearized optimal price-setting decision.

B.6 Substituting out $\tilde{p}_t$

Next, we follow a number of standard steps (e.g. Walsh (2017)) to solve for $\hat{\pi}_t$. From equation (A54) we have:

$$\begin{aligned}
\tilde{p}_t + \hat{\pi}_t &= (1-\beta_g\alpha)E_t\sum_{j=0}^{\infty}(\beta_g\alpha)^j\left(\frac{a_0\hat{y}_{t+j}+\hat{\mu}_{t+j}}{1+a_1}+\hat{\pi}_{t+j}\right), && \text{(A56)}\\
&= \frac{1-\beta_g\alpha}{1+a_1}(a_0\hat{y}_t+\hat{\mu}_t)+(1-\beta_g\alpha)\hat{\pi}_t\\
&\quad +\beta_g\alpha(1-\beta_g\alpha)E_t\sum_{j=0}^{\infty}(\beta_g\alpha)^j\left(\frac{a_0\hat{y}_{t+1+j}+\hat{\mu}_{t+1+j}}{1+a_1}+\hat{\pi}_{t+1+j}\right),\\
&= \frac{1-\beta_g\alpha}{1+a_1}(a_0\hat{y}_t+\hat{\mu}_t)+(1-\beta_g\alpha)\hat{\pi}_t+\beta_g\alpha E_t\left(\tilde{p}_{t+1}+\hat{\pi}_{t+1}\right) && \text{(A57)}
\end{aligned}$$

This equation relates the optimal relative price to the current-period marginal cost, current-period optimal markup, and the next-period expected optimal relative price. Subtracting $\hat{\pi}_t$ from both sides gives

$$\tilde{p}_t = \frac{1-\beta_g\alpha}{1+a_1}(a_0\hat{y}_t+\hat{\mu}_t)-\beta_g\alpha\hat{\pi}_t+\beta_g\alpha E_t\hat{\pi}_{t+1}+\beta_g\alpha E_t\tilde{p}_{t+1}. \tag{A58}$$

Substituting in the log-linearized law of motion for inflation (A39) and multiplying by $\frac{1-\alpha}{\alpha}$ gives

$$\left(\hat{\pi}_t-\hat{\pi}_{t-1}+v_t^{LT}\right) = \frac{1-\alpha}{\alpha}\frac{1-\beta_g\alpha}{1+a_1}(a_0\hat{y}_t+\hat{\mu}_t)-\beta_g\hat{\pi}_t+\beta_g E_t\hat{\pi}_{t+1} \tag{A59}$$

Solving for $\hat{\pi}_t$ gives the New Keynesian Phillips Curve (ignoring constants)

$$\hat{\pi}_t = \frac{\beta_g}{1+\beta_g}E_t\hat{\pi}_{t+1}+\frac{1}{1+\beta_g}\hat{\pi}_{t-1}+\kappa\hat{y}_t+\frac{\kappa}{a_0}\hat{\mu}_t-\frac{1}{1+\beta_g}v_t^{LT}, \tag{A60}$$

where the Phillips curve slope coefficient on $\hat{y}_t$ equals

$$\kappa = \frac{1}{1+\beta_g}\frac{1-\alpha}{\alpha}(1-\beta_g\alpha)\frac{a_0}{1+a_1}. \tag{A61}$$

Finally, we use that (up to a constant)

$$\begin{aligned}
\hat{\mu}_t &= \frac{1}{1-\theta}\varepsilon_{\theta,t} && \text{(A62)}\\
x_t &= \hat{y}_t, && \text{(A63)}\\
a_0 &= \omega, && \text{(A64)}\\
a_1 &= \omega\theta, && \text{(A65)}
\end{aligned}$$

and add the unit root component v_t^* to both sides of (A60) to obtain the log-linearized New Keynesian Phillips curve (29) in the main paper.

Note that the Phillips curve slope κ is identical to Woodford(1999, p.342) with three exceptions. First, β is replaced by β_g because we have equilibrium growth in our model. Second, the factor $\frac{1}{1+\beta_g}$ is new. This is due to indexing. Third, $a_0 = \omega$, whereas in Woodford (2003) the sensitivity of marginal cost with respect to aggregate log output is $\omega + \gamma$. This is due to our separation between the intertemporal consumption-savings trade-off and the intratemporal labor-leisure trade-off as in Greenwood, Hercowitz, and Huffman (1988). However, (Woodford (2003, p.341)) estimates a very small value for the curvature parameter from macroeconomic data of $\gamma = 0.16$, so the log-linearized Phillips curve in our model is not only qualitatively but also quantitatively in line with this prior work.

C Model Solution

C.1 Output gap and consumption relationships

With the assumption on the evolution of human capital (18), we can iterate to obtain

$$\begin{aligned} n_t &= \nu + n_{t-1} + (1-\phi)(1-\tau)l_{t-1}, && \text{(A66)} \\ &= \nu + n_{t-1} + (1-\phi)(y_{t-1} - a_{t-1}), && \text{(A67)} \\ &= \frac{\nu}{1-\phi} + (1-\phi)\sum_{j=0}^{\infty}\phi^j\left(y_{t-1-j} - a_{t-1-j}\right). && \text{(A68)} \end{aligned}$$

The deviation of output from the flexible-price equilibrium then equals (up to a constant):

$$\begin{aligned} x_t &= y_t - n_t - a_t, && \text{(A69)} \\ &= y_t - (1-\phi)\sum_{j=0}^{\infty}\phi^j\left(y_{t-1-j} - a_{t-1-j}\right) - a_t, && \text{(A70)} \\ &= c_t - (1-\phi)\sum_{j=0}^{\infty}\phi^j c_{t-1-j} - \sum_{j=0}^{\infty}\phi^j \Delta a_{t-j}, && \text{(A71)} \end{aligned}$$

i.e. equation (25) in the main paper. Because Δa_t is stationary and the geometric series ϕ^j has a finite sum, the deviation between the output gap x_t and stochastically detrended consumption is stationary. Consumption growth then takes the following simple form (up to a constant):

$$\begin{aligned} \Delta c_{t+1} &= (x_{t+1} + \sum_{j=0}^{\infty}\phi^j \Delta a_{t+1-j}) - \phi(x_t - \sum_{j=0}^{\infty}\phi^j \Delta a_{t-j}), && \text{(A72)} \\ &= x_{t+1} - \phi x_t + \Delta a_{t+1}, && \text{(A73)} \end{aligned}$$

i.e. equation (26) in the main paper.

C.2 Deriving the macro Euler equation

With the updating equation for log consumption growth (A73), the asset pricing Euler equation for the one-period real risk-free rate is given by:

$$r_t = \gamma E_t \Delta c_{t+1} + \gamma E_t \Delta \hat{s}_{t+1} - \frac{\gamma^2}{2}\left(1+\lambda(s_t)\right)^2 \sigma_c^2, \tag{A74}$$

$$= \gamma E_t \Delta c_{t+1} + \gamma(\theta_0 - 1)\hat{s}_t + \gamma\theta_1 x_t + \gamma\theta_2 x_{t-1} + \gamma\varepsilon_{s,t} - \frac{\gamma^2}{2}\left(1+\lambda(s_t)\right)^2 \sigma_c^2, \tag{A75}$$

$$= \gamma \Delta a_{t+1} + \gamma E_t x_{t+1} - \gamma\phi x_t + \gamma(\theta_0 - 1)\hat{s}_t + \gamma\theta_1 x_t + \gamma\theta_2 x_{t-1} + \gamma\varepsilon_{s,t} - \frac{\gamma^2}{2}\left(1+\lambda(s_t)\right)^2 \sigma_c^2$$

The sensitivity function has just the right form so that surplus consumption $\hat{s}_t$ drops out and (up to a constant):

$$r_t = \gamma \Delta a_{t+1} + \gamma E_t x_{t+1} - \gamma\phi x_t + \gamma\theta_1 x_t + \gamma\theta_2 x_{t-1} + \gamma\varepsilon_{s,t} \tag{A76}$$

Rearranging and continuing to ignore constants gives:

$$x_t = \frac{1}{\phi - \theta_1} E_t x_{t+1} + \frac{\theta_2}{\phi - \theta_1} x_{t-1} - \frac{1}{\gamma(\phi - \theta_1)}\left(r_t - \gamma \Delta a_{t+1}\right) + \frac{1}{\phi - \theta_1}\varepsilon_{s,t}. \tag{A77}$$

With the definition of the growth frictionless rate (20), this gives the log-linear Euler equation (27) in the main paper. Note that we have not made any approximations in the derivation of (27).

C.3 Solving for macroeconomic dynamics

We want to find a solution of the form

$$Y_t = BY_{t-1} + \Sigma v_t, \tag{A78}$$

where the matrix B is $[3 \times 3]$, the matrix Σ is $[3 \times 4]$, and the state vector Y_t is defined in equation (30) in the main paper. Throughout, we use Σ_v to denote the (diagonal) variance-covariance matrix of the vector of shocks, v_t. Substituting in for predictable productivity growth from equation (19) in main paper into (A77), We collect the log-linear equations describing the macroeconomic equilibrium dynamics:

$$x_t = f^x E_t x_{t+1} + \rho^x x_{t-1} - \psi\left(r_t - \gamma\rho^a r_t - \gamma\varepsilon_{s,t}\right), \tag{A79}$$

$$\pi_t = f^\pi E_t \pi_{t+1} + \rho^\pi \pi_{t-1} + \kappa x_t + v_{\pi,t}, \tag{A80}$$

$$i^* = \gamma^x x_t + \gamma^\pi \pi_t + (1-\gamma^\pi) v_t^*, \tag{A81}$$

$$i_t = \rho^i i_{t-1} + (1-\rho^i) i_t^* + v_{ST,t}, \tag{A82}$$

$$v_t^* = v_{t-1}^* + v_{LT,t} \tag{A83}$$

Writing this in terms of the elements of Y_t and using that $v_{x,t} = \gamma\psi\varepsilon_{s,t}$ gives

$$Y_{1,t} = f^x E_t Y_{1,t+1} + \rho^x Y_{1,t-1} - \psi(1-\gamma\rho^a)(Y_{3,t} - E_t Y_{2,t+1}) + v_{x,t}, \tag{A84}$$
$$Y_{2,t} = f^\pi E_t Y_{2,t+1} + \rho^\pi Y_{2,t-1} + \kappa Y_{1,t} + v_{\pi,t} - \rho^\pi v_{LT,t}, \tag{A85}$$
$$Y_{3,t} = \rho^i Y_{3,t-1} + (1-\rho^i)(\gamma^x Y_{1,t} + \gamma^\pi Y_{2,t}) + v_{ST,t} - \rho^i v_{LT,t}, \tag{A86}$$
$$v_t^* = v_{t-1}^* + v_{LT,t}. \tag{A87}$$

The same thing in matrix form:

$$0 = F E_t Y_{t+1} + G Y_t + H Y_{t-1} + M v_t,$$

where the matrices F, G and H are given by

$$F = \begin{bmatrix} f^x & \psi(1-\gamma\rho^a) & 0 \\ 0 & f^\pi & 0 \\ 0 & 0 & 0 \end{bmatrix},$$
$$G = \begin{bmatrix} -1 & 0 & -\psi(1-\gamma\rho^a) \\ \kappa & -1 & 0 \\ (1-\rho^i)\gamma^x & (1-\rho^i)\gamma^\pi & -1 \end{bmatrix},$$
$$H = \begin{bmatrix} \rho^x & 0 & 0 \\ 0 & \rho^\pi & 0 \\ 0 & 0 & \rho^i \end{bmatrix}.$$

The matrix M is $[3 \times 4]$ and equals:

$$M = \begin{bmatrix} 1 & 0 & 0 & 0 \\ 0 & 1 & 0 & -\rho^\pi \\ 0 & 0 & 1 & -\rho^i \end{bmatrix} \tag{A88}$$

Following Uhlig (1999), we solve for the generalized eigenvectors and eigenvalues of the matrix Ξ with respect to the matrix Δ, where

$$\Xi = \begin{bmatrix} -G & -H \\ I_3 & 0_3 \end{bmatrix}, \tag{A89}$$
$$\Delta = \begin{bmatrix} F & 0_3 \\ 0_3 & I_3 \end{bmatrix} \tag{A90}$$

To obtain a solution, we then pick three generalized eigenvalues $\lambda_1, \lambda_2, \lambda_3$ with generalized eigenvectors $[\lambda z_1', z_1']'$, $[\lambda_2 z_2', z_2]'$, and $[\lambda_3 z_3', z_3']'$. We denote the diagonal matrix of these eigenvalues by $\Lambda = diag\,(\lambda_1, \lambda_2, \lambda_3)$, and the matrix of the lower $[3 \times 1]$ portion of the eigenvectors by $\Omega = [z_1, z_2, z_3]$. The corresponding solutions for B and Σ are then given by:

$$B = \Omega\Lambda\Omega^{-1}, \tag{A91}$$
$$\Sigma = [FB + G]^{-1} M. \tag{A92}$$

In our empirical application, there exist exactly three generalized eigenvalues with absolute value less than one, and we pick the non-explosive solution corresponding to these three eigenvalues.

C.4 Rotated state vector

Our state space for solving for asset prices is five-dimensional: It consists of $\tilde{Z}_t$, which a scaled version of Y_t, the surplus consumption ratio relative to steady-state $\hat{s}_t$, and the lagged output gap x_{t-1}. The lagged output gap x_{t-1} is not actually needed as a state variable and we have verified that our numerical solutions for asset prices do not vary with x_{t-1}. Our code includes x_{t-1} as a state variable for legacy reasons.

We next describe the definition of $\tilde{Z}_t$. To simplify the numerical implementation of the asset pricing recursions, we require that shocks to the scaled state vector $\tilde{Z}_t$ are independent standard normal and that the first dimension of the scaled state vector is perfectly correlated with output gap innovations. This rotation facilitates the numerical analysis, because it is easier to integrate over independent random variables. Aligning the first dimension of the scaled state vector with output gap innovations (and hence surplus consumption innovations) helps, because it allows us to use a finer grid to integrate numerically over this crucial dimension over which asset prices are most non-linear.

If the scaled state vector equals $\tilde{Z}_t = AY_t$ for some invertible matrix A, the dynamics of $\tilde{Z}_t$ are given by:

$$\tilde{Z}_t = AY_t, \tag{A93}$$

$$\tilde{Z}_{t+1} = \underbrace{ABA^{-1}}_{\tilde{B}}\tilde{Z}_t + \underbrace{A\Sigma v_{t+1}}_{\epsilon_{t+1}}. \tag{A94}$$

We hence want a matrix, A, such that

$$Var\left(\epsilon_{t+1}\right) = A\Sigma\Sigma_v\Sigma' A', \tag{A95}$$

$$= \begin{bmatrix} 1 & 0 & 0 \\ 0 & 1 & 0 \\ 0 & 0 & 1 \end{bmatrix}. \tag{A96}$$

Finding such a matrix A should in general be possible, because the matrix M and therefore $\Sigma\Sigma_v\Sigma'$ hence generally have rank three. We require that the first dimension of ϵ_{t+1} is perfectly correlated with the consumption shock. We can therefore find the three rows of A using the following steps:

1. Set $A_1 = \frac{e_1}{\sqrt{e_1\Sigma\Sigma_v\Sigma' e_1'}}$.

2. We use the MATLAB function *null* to compute the null space of $A_1\Sigma\Sigma_v\Sigma'$. Let n_2 denote the first vector in *null* $\left(A_1\Sigma\Sigma_v\Sigma'\right)$. We then define the second row of A as the normalized version of n_2:

$$A_2 = \frac{n_2}{\sqrt{n_2\Sigma\Sigma_v\Sigma' n_2'}}. \tag{A97}$$

3. Let n_3 denote the first vector in $null\left(A_1\Sigma\Sigma_v\Sigma', A_2\Sigma\Sigma_v\Sigma'\right)$. We then define the third row of A as the normalized version of n_3:

$$A_3 \quad = \quad \frac{n_3}{\sqrt{n_3\Sigma\Sigma_v\Sigma' n_3'}}. \tag{A98}$$

It is then straightforward to verify that equation (A96) holds for

$$A \quad = \quad \begin{bmatrix} A_1 \\ A_2 \\ A_3 \end{bmatrix}. \tag{A99}$$

C.5 Asset pricing recursions

Before deriving the recursions for the numerical asset pricing computations, we derive a convenient form for the dynamics of the log surplus consumption ratio. We use e_i to denote a row vector with 1 in position i and zeros elsewhere. The matrix

$$\Sigma_M \quad = \quad e_1\Sigma \tag{A100}$$

denotes the loading of consumption innovations onto the vector of shocks v_t, where e_1 is a basis vector with a one in the first position and zeros everywhere else. The volatility of consumption surprises equals:

$$\sigma_c^2 \quad = \quad \Sigma_M\Sigma_v\Sigma_M'. \tag{A101}$$

To simplify notation, we define $\hat{s}_t$ as the log deviation of surplus consumption from its steady state. The dynamics of $\hat{s}_t$ are:

$$\hat{s}_t \quad = \quad s_t - \bar{s}, \tag{A102}$$

$$\hat{s}_t \quad = \quad \theta_0\hat{s}_{t-1} + \theta_1 x_{t-1} + \theta_2 x_{t-2} + \varepsilon_{s,t-1} + \lambda(\hat{s}_{t-1})\varepsilon_{c,t}, \tag{A103}$$

where with an abuse of notation we write:

$$\lambda(\hat{s}_t) \quad = \quad \lambda_0\sqrt{1-2\hat{s}_t} - 1, \hat{s}_t \leq s_{max} - \bar{s}, \tag{A104}$$

$$\lambda(\hat{s}_t) \quad = \quad 0, \hat{s}_t \geq s_{max} - \bar{s}. \tag{A105}$$

The steady-state surplus consumption sensitivity equals:

$$\lambda_0 \quad = \quad \frac{1}{\bar{S}}. \tag{A106}$$

In our calculations of asset prices, we repeatedly substitute out expected log SDF growth, which equals:

$$E_t\left[m_{t+1}\right] \quad = \quad \log\beta - \gamma E_t\Delta\hat{s}_{t+1} - \gamma E_t\Delta c_{t+1}, \tag{A107}$$

$$\quad = \quad -r_t - \frac{\gamma}{2}(1-\theta_0)(1-2\hat{s}_t). \tag{A108}$$

We often combine this with $r_t = \bar{r} + (e_3 - e_2 B) Z_t$ and $\hat{r}_t = (e_3 - e_2 B) Z_t$.

Including the constant, consumption growth is given by:

$$\Delta c_{t+1} = g + x_{t+1} - \phi x_t + \Delta a_{t+1}, \tag{A109}$$

$$= g + x_{t+1} - \phi x_t + \rho^a \hat{r}_t. \tag{A110}$$

The steady state real short-term interest rate at $x_t = 0$ and $s_t = \bar{s}$ is the same as in Campbell and Cochrane (1999):

$$\bar{r} = \gamma g - \frac{1}{2}\gamma^2 \sigma_c^2 / \bar{S}^2 - log(\beta). \tag{A111}$$

The updating rule for the log surplus consumption ratio can then be written in terms of the state variables as:

$$\hat{s}_{t+1} = \hat{s}_t + E_t \Delta \hat{s}_{t+1} + \lambda(\hat{s}_t)\varepsilon_{c,t+1}, \tag{A112}$$

$$= \hat{s}_t - E_t \Delta \hat{c}_{t+1} + \frac{1}{\gamma}\left(\log\beta + \hat{r}_t + \bar{r} + \frac{\gamma}{2}(1-\theta_0)(1-2\hat{s}_t)\right) + \lambda(\hat{s}_t)\varepsilon_{c,t+1}, \tag{A113}$$

$$= \theta_0 \hat{s}_t + \frac{1}{\gamma}(e_3 - e_2 B) A^{-1}\tilde{Z}_t - e_1 [B - \phi I] A^{-1} \tilde{Z}_t - \rho^a \hat{r}_t + \lambda(\hat{s}_t)\varepsilon_{c,t+1}, \tag{A114}$$

$$= \theta_0 \hat{s}_t + \frac{1}{\gamma}(1 - \gamma\rho^a)(e_3 - e_2 B) A^{-1}\tilde{Z}_t - e_1 [B - \phi I] A^{-1} \tilde{Z}_t + \lambda(\hat{s}_t)\varepsilon_{c,t+1}. \tag{A115}$$

C.5.1 Recursion for zero-coupon consumption claims

We now derive the recursion for zero-coupon consumption claims in terms of state variables $\tilde{Z}_t$, $\hat{s}_t$ and x_{t-1}. Let P^c_{nt}/C_t denote the price-dividend ratio of a zero-coupon claim on consumption at time $t+n$. The outline of our strategy here is that we first derive an analytic expression for the price-dividend ratio for P^c_{1t}/C_t. For $n \geq 1$ we guess and verify recursively that there exists a function $F_n(\tilde{Z}_t, \hat{s}_t, x_{t-1})$, such that

$$\frac{P^c_{nt}}{C_t} = F_n\left(\tilde{Z}_t, \hat{s}_t, x_{t-1}\right). \tag{A116}$$

The ex-dividend price-consumption ratio for a claim to all future consumption is then given by

$$\frac{P_t}{C_t} = F\left(\tilde{Z}_t, \hat{s}_t, x_{t-1}\right), \tag{A117}$$

where we define

$$F\left(\tilde{Z}_t, \hat{s}_t, x_{t-1}\right) = \sum_{n=1}^{\infty} F_n\left(\tilde{Z}_t, \hat{s}_t, x_{t-1}\right). \tag{A118}$$

We now derive the recursion of zero-coupon consumption claims in terms of state variables $\tilde{Z}_t$ and $\hat{s}_t$. The one-period zero coupon price-consumption ratio solves:

$$\frac{P^c_{1,t}}{C_t} = E_t\left[\frac{M_{t+1}C_{t+1}}{C_t}\right] \tag{A119}$$

We simplify

$$\frac{M_{t+1}C_{t+1}}{C_t} = \beta exp\left(E_t m_{t+1} + E_t \Delta c_{t+1} - \gamma(\hat{s}_{t+1} - E_t s_{t+1}) - (\gamma-1)(c_{t+1} - E_t c_{t+1})\right).$$

Using the notation $f_n = \log(F_n)$, this gives the log one-period price-consumption ratio as:

$$\begin{aligned} f_1\left(\tilde{Z}_t, \hat{s}_t, x_{t-1}\right) &= -r_t - \frac{\gamma}{2}(1-\theta_0)(1-2\hat{s}_t) + g + \Delta a_{t+1} + E_t x_{t+1} - \phi x_t \\ &\quad + \frac{1}{2}\left(\gamma\lambda(\hat{s}_t) + (\gamma-1)\right)^2 \sigma_c^2, \quad \text{(A120)} \\ &= g + e_1\left[B - \phi I\right] A^{-1}\tilde{Z}_t + \frac{1}{2}\left(\gamma\lambda(\hat{s}_t) + (\gamma-1)\right)^2 \sigma_c^2 \\ &\quad -\bar{r} - (1-\rho^a)\left(e_3 - e_2 B\right) A^{-1}\tilde{Z}_t - \frac{\gamma}{2}(1-\theta_0)(1-2\hat{s}_t) \quad \text{(A121)} \end{aligned}$$

Next, we solve for f_n, $n \geq 2$ iteratively. Note that:

$$\frac{P^c_{nt}}{C_t} = \mathbb{E}_t\left[\frac{M_{t+1}C_{t+1}}{C_t}\frac{P^c_{n-1,t+1}}{C_{t+1}}\right] = \mathbb{E}_t\left[\frac{M_{t+1}C_{t+1}}{C_t}F_{n-1}\left(\tilde{Z}_{t+1}, \hat{s}_{t+1}, x_t\right)\right] \quad \text{(A122)}$$

This gives the following expression for f_n:

$$\begin{aligned} f_n(\tilde{Z}_t, \hat{s}_t, \hat{r}_{t-1}) &= \log\Big[\mathbb{E}_t\Big[\exp\Big(g + e_1[B - \phi I]A^{-1}\tilde{Z}_t \\ &\quad -\bar{r} - (1-\rho^a)(e_3 - e_2 B)A^{-1}\tilde{Z}_t - \frac{\gamma}{2}(1-\theta_0)(1-2\hat{s}_t) \\ &\quad -(\gamma(1+\lambda(\hat{s}_t)) - 1)\sigma_c \epsilon_{1,t+1} \\ &\quad + f_{n-1}(\tilde{Z}_{t+1}, \hat{s}_{t+1}, \hat{r}_t)\Big)\Big]\Big]. \quad \text{(A123)} \end{aligned}$$

Here, $\epsilon_{1,t+1}$ denotes the first dimension of the shock ϵ_{t+1}.

C.5.2 Recursion for zero-coupon bond prices

We use $P^{\$}_{n,t}$ and $P_{n,t}$ to denote the prices of nominal and real n-period zero-coupon bonds. The strategy is to develop analytic expressions for one- and two-period bond prices. We then guess and verify recursively that the prices of real and nominal zero-coupon bonds with maturity $n \geq 2$ can be written in the following form:

$$\begin{aligned} P_{n,t} &= B_n(\tilde{Z}_t, \hat{s}_t, x_{t-1}), \quad \text{(A124)} \\ P^{\$}_{n,t} &= exp(-n v^*_t) B^{\$}_n(\tilde{Z}_t, \hat{s}_t, x_{t-1}), \quad \text{(A125)} \end{aligned}$$

where $B_n(\tilde{Z}_t, \hat{s}_t, x_{t-1})$ and $B^{\$}_n(\tilde{Z}_t, \hat{s}_t, x_{t-1})$ are functions of the state variables. As discussed in the main paper, we assume that the short-term nominal interest rate contains no risk premium, so the one-period log nominal interest rate equals $i_t = r_t + E_t\pi_{t+1}$. Taking account of the constants, one-period bond prices equal:

$$\begin{aligned} P^{\$}_{1,t} &= \exp(-Y_{3,t} - v^*_t - \bar{r}), \quad \text{(A126)} \\ P_{1,t} &= \exp(-Y_{3,t} + \mathbb{E}_t Y_{2,t+1} - \bar{r}). \quad \text{(A127)} \end{aligned}$$

We next solve for longer-term bond prices including risk premia. Substituting in (A126) into the bond-pricing recursion gives:

$$\begin{aligned} P^{\$}_{2,t} &= \mathbb{E}_t\left[M_{t+1}P^{\$}_{1,t+1}\exp(-v^*_{t+1}-Y_{2,t+1})\right] && \text{(A128)}\\ &= \mathbb{E}_t\left[M_{t+1}\exp(-Y_{3,t+1}-2v^*_{t+1}-Y_{2,t+1}-\bar{r})\right]. && \text{(A129)}\end{aligned}$$

We can now verify that the two-period nominal bond price takes the form (A125):

$$\begin{aligned} B^{\$}_2(\tilde{Z}_t,\hat{s}_t,x_{t-1}) &= \exp\left(E_t\left(m_{t+1}-Y_{3,t+1}-Y_{2,t+1}\right)-\bar{r}\right)\\ &\times\mathbb{E}_t\left[\exp\left(\left(-\gamma\left(\lambda(\hat{s}_t)+1\right)\Sigma_M-\underbrace{[(e_2+e_3)\Sigma+2e_4]}_{v_{\$}}\right)v_{t+1}\right)\right]. \end{aligned} \tag{A130}$$

Here, we define the vector $v_{\$}$ to simplify notation. The random walk component of inflation v^*_t does not appear in (A130), because $B^{\$}_2$ is already scaled by $exp(-2v^*_t)$ by definition (A125). Taking logs, substituting out for $E_t m_{t+1}$, and using the definition for the sensitivity function $\lambda(\hat{s}_t)$, we get:

$$\begin{aligned} b^{\$}_2 &= -e_3[I+B]A^{-1}\tilde{Z}_t+\frac{1}{2}v_{\$}\Sigma_v v_{\$}{\prime}\\ &\quad+\gamma\left(\lambda(\hat{s}_t)+1\right)\Sigma_M\Sigma_v v'_{\$}-2\bar{r}. \end{aligned} \tag{A131}$$

We similarly solve for two-period real bond prices in closed form:

$$\begin{aligned} P_{2,t} &= \exp\left(E_t\left(m_{t+1}-Y_{3,t+1}+Y_{2,t+2}\right)-\bar{r}\right)\\ &\times\mathbb{E}_t\left[\exp\left((-\gamma(\lambda(\hat{s}_t)+1)\Sigma_M-\underbrace{(e_3-e_2B)\Sigma}_{v_r})v_{t+1}\right)\right] \end{aligned} \tag{A132}$$

We define the vector v_r to simplify notation. Taking logs, substituting out for $E_t m_{t+1}$, and using the definition for $\lambda(\hat{s}_t)$ gives:

$$b_2(\tilde{Z}_t,\hat{s}_t,x_{t-1}) = -(e_3-e_2B)\left[I+B\right]A^{-1}\tilde{Z}_t+\frac{1}{2}v_r\Sigma_v v'_r+\gamma\left(\lambda(\hat{s}_t)+1\right)\Sigma_M\Sigma_v v'_r-2\bar{r}. \tag{A133}$$

For $n\geq 3$, we repeatedly substitute out for $E_t m_{t+1}$ to obtain the following recursion for real bond prices:

$$\begin{aligned} B_n(\tilde{Z}_t,\hat{s}_t,x_{t-1}) &= \mathbb{E}_t\left[\exp\left(m_{t+1}+b_{n-1}(\tilde{Z}_{t+1},\hat{s}_{t+1},x_t)\right)\right]\\ &= \mathbb{E}_t\Big[\exp\Big(-\bar{r}-(e_3-e_2B)A^{-1}\tilde{Z}_t-\frac{\gamma}{2}(1-\theta_0)(1-2\hat{s}_t)\\ &\quad-\gamma(1+\lambda(\hat{s}_t))\sigma_c\epsilon_{1,t+1}+b_{n-1}(\tilde{Z}_{t+1},\hat{s}_{t+1},x_t)\Big)\Big]. \end{aligned} \tag{A134}$$

The recursion for nominal bond prices with $n \geq 3$ is similar. It is complicated by the fact that we need to integrate over long-term monetary policy shocks, which are not necessarily spanned by ϵ_{t+1}:

$$B_n^{\$}(\tilde{Z}_t, \hat{s}_t, x_{t-1}) = \mathbb{E}_t \left[\exp \left(m_{t+1} - Y_{2,t+1} - n v_{t+1}^{LT} + b_{n-1}^{\$}(\tilde{Z}_{t+1}, \hat{s}_{t+1}, x_t) \right) \right]. \tag{A135}$$

To reduce the number of dimensions along which we need to integrate numerically, we split v_{t+1}^{LT} into a component that is spanned by ϵ_{t+1} plus an orthogonal shock. This is useful because we can then use analytic expressions to integrate over the orthogonal component. We use the standard expression for conditional distributions of multivariate normal random variables. The distribution of v_{t+1}^{LT} conditional on ϵ_{t+1} is normal with:

$$v_{t+1}^{LT} | \epsilon_{t+1} \sim N \left(\underbrace{(A\Sigma\Sigma_v e_4')'}_{vec_*} \epsilon_{t+1}, \underbrace{(\sigma_{LT})^2 - (A\Sigma\Sigma_v e_4')'(A\Sigma\Sigma_v e_4')}_{\sigma_\perp^2} \right). \tag{A136}$$

We then write v_t^{LT} as the sum of two independent shocks:

$$v_{t+1}^{LT} = vec^* \epsilon_{t+1} + \epsilon_{t+1}^{\perp}, \tag{A137}$$

where $\epsilon_{t+1}^{\perp}$ is defined as

$$\epsilon_{t+1}^{\perp} := v_{t+1}^{LT} - vec^* \epsilon_{t+1} \tag{A138}$$

We integrate analytically over $\epsilon_{t+1}^{\perp}$ in equation (A139):

$$\begin{aligned} B_n^{\$}(\tilde{Z}_t, \hat{s}_t, x_{t-1}) &= \mathbb{E}_t \left[\exp \left(m_{t+1} - Y_{2,t+1} - n vec^* \epsilon_{t+1} + \frac{n^2}{2}(\sigma_\perp)^2 + b_{n-1}^{\$}(\tilde{Z}_{t+1}, \hat{s}_{t+1}, B^{\$} x_t) \right) \right], \\ &= \mathbb{E}_t \Bigg[\exp \Bigg(-\bar{r} - e_3 A^{-1} \tilde{Z}_t - \frac{\gamma}{2}(1 - \theta_0)(1 - 2\hat{s}_t) \\ &\quad -(\gamma(1 + \lambda(\hat{s}_t))\sigma_c + \underbrace{e_2 A^{-1} e_1'}_{vpi_1} + n vec^* e_1')\epsilon_{1,t+1} \\ &\quad - \left(\underbrace{e_2 A^{-1} e_2'}_{vpi_2} + n vec^* e_2' \right) \epsilon_{2,t+1} \\ &\quad + \frac{n^2}{2}(\sigma_\perp)^2 + b_{n-1}^{\$}(\tilde{Z}_{t+1}, \hat{s}_{t+1}, x_t) \Bigg) \Bigg]. \end{aligned} \tag{A139}$$

We define the vectors vpi_1 and vpi_2 as given above to avoid computing them repeatedly in our numerical algorithm.

C.5.3 Computing returns

The log return on the consumption claim equals:

$$r^c_{t+1} = \log\left(\frac{P^c_{t+1} + C_{t+1}}{P^c_t}\right), \tag{A140}$$

$$= \Delta c_{t+1} + \log\left(\frac{1 + \frac{P^c_{t+1}}{C_{t+1}}}{\frac{P^c_t}{C_t}}\right). \tag{A141}$$

Real and nominal log bond yields equal:

$$y_{n,t} = -\frac{1}{n} b_{n,t}, \tag{A142}$$

$$y^{\$}_{n,t} = -\frac{1}{n} b^{\$}_{n,t} + \pi^*_t. \tag{A143}$$

Real log bond returns equal:

$$r_{n,t+1} = b_{n-1,t+1} - b_{n,t}. \tag{A144}$$

Nominal log bond returns equal:

$$r^{\$}_{n,t+1} = b^{\$}_{n-1,t+1} - b^{\$}_{n,t} - (n-1)v^*_{t+1} + nv^*_t. \tag{A145}$$

Real and nominal bond log excess returns then equal:

$$xr_{n,t+1} = r_{n,t+1} - r_t, \tag{A146}$$

$$xr^{\$}_{n,t+1} = r^{\$}_{n,t+1} - i_t. \tag{A147}$$

C.5.4 Levered stock prices and returns

We note that the price of the levered equity claim is δP^c_t, so the price-dividend ratio equals:

$$\frac{P^\delta_t}{D^\delta_t} = \delta \frac{C_t}{D^\delta_t} \frac{P^c_t}{C_t}. \tag{A148}$$

Using the expression

$$D^\delta_{t+1} = P^c_{t+1} + C_{t+1} - (1-\delta)P^c_t \exp(r_t) - \delta P^c_t, \tag{A149}$$

and

$$P^\delta_t = \delta P^c_t \tag{A150}$$

gives the gross return on levered stocks:

$$\left(1+R^{\delta}_{t+1}\right) = \frac{D^{\delta}_{t+1}+P^{\delta}_{t+1}}{P^{\delta}_{t}}, \tag{A151}$$
$$= \frac{1}{\delta}\frac{P^{c}_{t+1}+C_{t+1}-(1-\delta)P^{c}_{t}exp(r_t)}{P^{c}_{t}}, \tag{A152}$$
$$= \frac{1}{\delta}\left(1+R^{c}_{t+1}\right)-\frac{1-\delta}{\delta}exp\left(r_t\right). \tag{A153}$$

Log stock excess returns then equal:

$$xr^{\delta}_{t+1} = r^{\delta}_{t+1}-r_t. \tag{A154}$$

To mimic firms' dividend smoothing in the data, we report simulated moments for the price of equities dividend by dividends smoothed over the past 64 quarters:

$$P^{\delta}_{t}/\left(\frac{1}{64}(D^{\delta}_{t}+D^{\delta}_{t-1}+...+D^{\delta}_{t-63})\right). \tag{A155}$$

C.6 Risk-premium decomposition

We use the superscript ^{rn} for risk-neutral, superscript ^{cf} for cash flow, and ^{rp} for risk premium. Risk-neutral valuations are expected cash flows discounted with the risk-neutral discount factor, that is consistent with equilibrium dynamics for the real interest rate:

$$M^{rn}_{t+1} = exp(-r_t). \tag{A156}$$

C.6.1 Risk-neutral zero-coupon bond prices

We use analogous recursions to solve for risk-neutral bond prices. One-period risk-neutral bond prices are given exactly as before by equations (A126) and (A127). For $n>1$, we guess and verify that the prices of real and nominal risk-neutral zero-coupon bonds with maturity n can be written in the following form

$$P^{rn}_{n,t} = B^{rn}_{n}(\tilde{Z}_t,\hat{s}_t,x_{t-1}), \tag{A157}$$
$$P^{\$,rn}_{n,t} = exp(-nv^{*}_{t})B^{\$,rn}_{n}(\tilde{Z}_t,\hat{s}_t,x_{t-1}). \tag{A158}$$

for some functions $B^{rn}_{n}(\tilde{Z}_t,\hat{s}_t,x_{t-1})$ and $B^{\$,rn}_{n}(\tilde{Z}_t,\hat{s}_t,x_{t-1})$.

We derive the two-period risk-neutral nominal bond price analytically:

$$P^{\$,rn}_{2,t} = exp(-r_t)\mathbb{E}_t\left[P^{\$,rn}_{1,t+1}\exp(-v^{*}_{t+1}-Y_{2,t+1})\right] \tag{A159}$$
$$= exp(-r_t)\mathbb{E}_t\left[\exp(-Y_{3,t+1}-2v^{*}_{t+1}-Y_{2,t+1}-\bar{r})\right]. \tag{A160}$$

We can hence verify that the two-period risk-neutral nominal bond price takes the form (A125)

$$b^{\$,rn}_{2} = -e_3\left[I+B\right]A^{-1}\tilde{Z}_t+\frac{1}{2}v_{\$}\Sigma_u v_{\$}\prime-2\bar{r} \tag{A161}$$

Here, the vector $v_{\$}$ is identical to the case with risk aversion. Comparing expressions (A161) and (A131) shows that they agree when $\gamma = 0$. We similarly solve for 2-period real bond prices in closed form:

$$P_{2,t}^{rn} = \exp\left(-Y_{3,t} + \mathbb{E}_t Y_{2,t+1} - \bar{r}\right) \times \exp\left(\mathbb{E}_t\left(-Y_{3,t+1} + \mathbb{E}_{t+1} Y_{2,t+2} - \bar{r}\right)\right) \times \mathbb{E}_t\left[\exp\left(-\underbrace{(e_3 - e_2 B)\Sigma}_{v_r} v_{t+1}\right)\right]. \quad \text{(A162)}$$

The vector v_r is again identical to the case with risk aversion. Taking logs gives:

$$b_2^{rn}(\tilde{Z}_t, \hat{s}_t, x_{t-1}) = -(e_3 - e_2 B)\left[I + B\right] A^{-1}\tilde{Z}_t + \frac{1}{2} v_r \Sigma_u v_r' - 2\bar{r}. \quad \text{(A163)}$$

We note that the risk-neutral bond prices (A163) and bond prices with risk aversion (A133) are identical when the utility curvature parameter γ equals zero.

For $n \geq 3$ the n-period risk neutral real bond price B_n^{rn} satisfies the recursion:

$$B_n^{rn}(\tilde{Z}_t, \hat{s}_t, x_{t-1}) = \mathbb{E}_t\left[\exp\left(-\bar{r} - (e_3 - e_2 B)A^{-1}\tilde{Z}_t + b_{n-1}(\tilde{Z}_{t+1}, \hat{s}_{t+1}, x_t)\right)\right] \quad \text{(A164)}$$

We obtain a similar recursion for risk-neutral nominal bond prices:

$$B_n^{\$,rn}(\tilde{Z}_t, \hat{s}_t, x_{t-1}) = \mathbb{E}_t\left[\exp\left(Y_{3,t} + \mathbb{E}_t Y_{2,t+1} - \bar{r} - Y_{2,t+1} - n v_{t+1}^* + b_{n-1}^{\$}(\tilde{Z}_{t+1}, \hat{s}_{t+1}, x_t)\right)\right].$$

We again use the decomposition $v_{t+1}^* = vec^* \epsilon_{t+1} + \epsilon_{t+1}^{\perp}$ from Section C.5.2 to reduce the dimensionality of the numerical integration:

$$\begin{aligned} B_n^{\$,rn}(\tilde{Z}_t, \hat{s}_t, x_{t-1}) &= \mathbb{E}_t\left[\exp\left(-Y_{3,t} + \mathbb{E}_t Y_{2,t+1} - \bar{r} - Y_{2,t+1} - n \cdot vec^* \epsilon_{t+1} + \frac{n^2}{2}(\sigma^{\perp})^2 \right.\right. \\ &\quad \left.\left. + b_{n-1}^{\$}(\tilde{Z}_{t+1}, \hat{s}_{t+1}, x_t)\right)\right], \quad \text{(A165)} \\ &= \mathbb{E}_t\left[\exp\left(-\bar{r} - e_3 A^{-1}\tilde{Z}_t - (\underbrace{e_2 A^{-1} e_1'}_{vpi_1} + n \cdot vec^* e_1')\epsilon_{1,t+1} \right.\right. \\ &\quad \left.\left. - \left(\underbrace{e_2 A^{-1} e_2'}_{vpi_2} + n \cdot vec^* e_2'\right)\epsilon_{2,t+1} + \frac{n^2}{2}(\sigma^{\perp})^2 + b_{n-1}^{\$}(\tilde{Z}_{t+1}, \hat{s}_{t+1}, x_t)\right)\right]. \quad \text{(A166)} \end{aligned}$$

C.6.2 Risk-neutral zero-coupon consumption claims

Next, we derive recursive solutions for the risk-neutral prices of zero-coupon consumption claims. Let $P_{nt}^{c,rn}/C_t$ denote the risk-neutral price-dividend ratio of a zero-coupon claim on consumption at time $t+n$. The risk-neutral price-consumption ratio of a claim to the entire stream of future consumption equals:

$$\frac{P_t^{c,rn}}{C_t} = \sum_{n=1}^{\infty} \frac{P_{nt}^{c,rn}}{C_t}. \tag{A167}$$

For $n \geq 1$, we guess and verify there exists a function $F_n^{rn}(\tilde{Z}_t, \hat{s}_t, x_{t-1})$, such that

$$\frac{P_{nt}^{c,rn}}{C_t} = F_n^{rn}\left(\tilde{Z}_t, \hat{s}_t, x_{t-1}\right). \tag{A168}$$

We start by deriving the analytic expression for F_1^{rn}. The one-period risk-neutral zero-coupon price-consumption ratio solves

$$\frac{P_{1,t}^{c,rn}}{C_t} = exp\left(-Y_{3,t} + \mathbb{E}_t Y_{2,t+1} - \bar{r}\right) \mathbb{E}_t \left[\frac{C_{t+1}}{C_t}\right] \tag{A169}$$

Using (26) to substitute for consumption growth, we can derive the following analytic expression for f_1^{rn}:

$$f_1^{rn}(\tilde{Z}_t, \hat{s}_t, x_{t-1}) = -(1-\rho^a)\left(e_3 - e_2 B\right) A^{-1}\tilde{Z}_t - \bar{r} + g + e_1[B - \phi I]A^{-1}\tilde{Z}_t + \frac{1}{2}\sigma_c^2. \tag{A170}$$

Next, we solve for f_n, $n \geq 2$ iteratively:

$$\frac{P_{nt}^{c,rn}}{C_t} = exp\left(-Y_{3,t} + \mathbb{E}_t Y_{2,t+1} - \bar{r}\right) \mathbb{E}_t \left[\frac{C_{t+1}}{C_t} F_{n-1}^{rn}\left(\tilde{Z}_{t+1}, \hat{s}_{t+1}, x_t\right)\right] \tag{A171}$$

This gives the following expression for f_n^{rn}:

$$\begin{aligned} f_n^{rn}(\tilde{Z}_t, \hat{s}_t, x_{t-1}) = {} & \log\left[\mathbb{E}_t\left[\exp\left(-(1-\rho^a)\left(Y_{3,t} + \mathbb{E}_t Y_{2,t+1}\right) - \bar{r} + g - \phi x_t + \mathbb{E}_t x_{t+1} + \sigma_c \epsilon_{1,t+1}\right.\right.\right. \\ & \left.\left.\left. + f_{n-1}^{rn}(\tilde{Z}_{t+1}, \hat{s}_{t+1}, x_t)\right)\right]\right]. \end{aligned} \tag{A172}$$

Finally, we re-write $f_{n,t}^{rn}$ as an expectation involving $f_{n-1,t+1}^{rn}$, the state variables $\tilde{Z}_t$, and period $t+1$ shocks:

$$\begin{aligned} f_n^{rn}(\tilde{Z}_t, \hat{s}_t, x_{t-1}) = {} & \log\left[\mathbb{E}_t\left[\exp\left(g + e_1[B - \phi I]A^{-1}\tilde{Z}_t - \bar{r} - (1-\rho^a)\left(e_3 - e_2 B\right) A^{-1}\tilde{Z}_t + \right.\right.\right. \\ & \left.\left.\left. + \sigma_c \epsilon_{1,t+1} + f_{n-1}^{rn}(\tilde{Z}_{t+1}, \hat{s}_{t+1}, x_t)\right)\right]\right]. \end{aligned} \tag{A173}$$

C.6.3 Risk-neutral returns

We plug risk-neutral price-consumption ratios and bond prices into equations (A141) through (A147). This gives risk-neutral returns on the consumption claim, risk-neutral log excess bond returns, and risk-neutral bond yields. We then substitute risk-neutral returns on the consumption claim into (A153)-(A154) to obtain risk-neutral log excess stock returns.

C.7 Modeling FOMC High-Frequency Asset Prices

In order to simulate high-frequency changes in stocks and bonds around FOMC announcements, we decompose the quarterly shock into a pre-FOMC and an FOMC component, which are assumed to be uncorrelated

$$v_t = v_t^{pre} + v_t^{FOMC}. \tag{A174}$$

We therefore effectively model FOMC dates as occurring always at the end of the quarter, because that is the only date when we compute asset prices. The variance-covariance matrix of shocks released prior to the FOMC announcement is

$$\Sigma_v^{pre} = \Sigma_v - diag\left([\sigma_x^{FOMC}, \sigma_\pi^{FOMC}, \sigma_{ST}^{FOMC}, \sigma_{LT}^{FOMC}]\right). \tag{A175}$$

We then split the rotated ϵ_t shock similarly according to

$$\epsilon_t^{pre} = A\Sigma v_t^{pre}, \tag{A176}$$
$$\epsilon_t^{FOMC} = A\Sigma v_t^{FOMC}. \tag{A177}$$

The aggregate dynamics and asset pricing solution are of course unchanged to before, because the distribution of quarterly fundamental shocks v_t is unchanged. But splitting it into two independent shocks allows us to differentiate asset prices before vs. after the FOMC shock v_t^{FOMC}.

We compute pre-FOMC asset prices very simply at the expected quarter t state vector before the FOMC shock is realized. The expected pre-FOMC state variables plus consumption are given by

$$\tilde{Z}_t^{pre} = \tilde{P}\tilde{Z}_{t-1} + \epsilon_t^{pre}, \tag{A178}$$
$$Y_t^{pre} = PY_{t-1} + A^{-1}\epsilon_t^{pre}, \tag{A179}$$
$$\hat{s}_t^{pre} = \theta_0\hat{s}_{t-1} + \theta_1 Y_{1,t-1} + \theta_2 Y_{1,t-2} + ...\lambda(\hat{s}_{t-1}, \bar{S})\sigma_c\epsilon_{1,t}^{pre}, \tag{A180}$$
$$c_t^{pre} = g + c_{t-1} + (Y_{1,t}^{pre} - \phi Y_{1,t-1}), \tag{A181}$$
$$v_t^{*,pre} = v_{t-1}^* + v_t^{LT,pre}. \tag{A182}$$

We compute pre-FOMC stock and bond prices by substituting the pre-FOMC state vector into the solutions from the asset pricing value function iterations:

$$\frac{P_t^{pre}}{C_t^{pre}} = F\left(\tilde{Z}_t^{pre}, \hat{s}_t^{pre}, x_{t-1}\right), \tag{A183}$$
$$P_{n,t}^{\$,pre} = exp\left(-nv_t^{*,pre}\right) B_n^{\$}\left(\tilde{Z}_t^{pre}, \hat{s}_t^{pre}, x_{t-1}\right), \tag{A184}$$
$$P_{n,t}^{pre} = B_n\left(\tilde{Z}_t^{pre}, \hat{s}_t^{pre}, x_{t-1}\right) \tag{A185}$$

The pre-FOMC nominal and real log bond yields are then given by

$$y_{n,t}^{\$,pre} = -n\log\left(P_{n,t}^{\$,pre}\right), \tag{A186}$$
$$y_{n,t}^{pre} = -n\log\left(P_{n,t}^{pre}\right). \tag{A187}$$

Pre-FOMC breakeven is computed as

$$breakeven^{pre}_{n,t} = y^{\$,pre}_{n,t} - y^{pre}_{n,t}. \tag{A188}$$

We then compute simulated changes in the short-term nominal interest rate, as well as long-term bond yields and breakeven around FOMC announcements

$$\Delta i^{FOMC}_t = (Y_{3,t} + v^*_t) - \left(Y^{pre}_{3,t} + v^{*,pre}_t\right), \tag{A189}$$

$$\Delta y^{\$,FOMC}_{n,t} = y^{\$}_{n,t} - y^{\$,pre}_{n,t}, \tag{A190}$$

$$\Delta y^{FOMC}_{n,t} = y_{n,t} - y^{pre}_{n,t}, \tag{A191}$$

$$\Delta breakeven^{FOMC}_{n,t} = breakeven_{n,t} - breakeven^{pre}_{n,t}. \tag{A192}$$

Stock returns around the FOMC date are computed assuming that no consumption takes place during the FOMC interval (equivalently, the FOMC intervals is infinitesimal), so

$$r^{c,FOMC}_t = \log\left(exp(c_t - c^{pre}_t) \frac{\frac{P^c_t}{C_t}}{\frac{P^{c,pre}_t}{C^{pre}_t}} \right). \tag{A193}$$

The levered return around the FOMC date then is

$$r^{\delta,FOMC}_t = log((1/\delta) exp(r^{c,FOMC}_t) - ((1-\delta)/\delta)), \tag{A194}$$

which follows from using the standard formula for levered stock returns while setting the real interest rate and consumption to zero, because the FOMC interval is infinitesimal.

D Solving for Asset Prices numerically

We evaluate asset prices by iterating on a grid for the state vector as in Campbell, Pflueger, and Viceira (2020) building on Wachter (2005). Other numerical methodologies are faster, but their cost is that they cannot replicate the economic properties of Wachter (2005)'s numerical solution for Campbell-Cochrane. In unreported results, we verified that analytic linear approximations to the sensitivity function λ (e.g. Lopez, López-Salido, and Vazquez-Grande 2015), numerical higher-order perturbation methods using Dynare (Rudebusch and Swanson 2008), and global projection methods give solutions for Campbell-Cochrane that are economically very different from Wachter (2005)'s numerical solution.

Other approaches in the literature are also not appropriate for our problem. While Chen (2017) solves a model with habit and production using global projection and perturbation methods, his model features a linear sensitivity function and heteroskedastic consumption. By contrast, we have homoskedastic consumption and a highly nonlinear sensitivity function. Similarly, affine term structure models, such as Dai and Singleton (2000), generate affine relations between risk premia and state variables by assuming analytically convenient functional forms for the pricing kernel. In contrast to models that assume more convenient pricing kernels, our preferences are consistent with the standard log-linear New Keynesian consumption Euler equation and generate conditionally homoskedastic macroeconomic dynamics.

While iterating on a grid is significantly slower than perturbation or global projection methods, it is not prohibitively so. Our MATLAB algorithm for solving the asset pricing recursions (described in Section D.1) takes 94 seconds to run on a Lenovo X280 laptop with an i7-8650U CPU. Simulating the model (described in Section D.2) takes 35 seconds. The risk-neutral asset pricing recursions and simulating the risk-neutral stock returns take an additional 88 seconds and 37 seconds.

D.1 Implementing the asset pricing recursions

We implement the recursions in Sections C.5.1 and C.5.2 numerically through value function iteration on a grid. We solve for the functions f_n, b_n, and $b_n^{\$}$ using value function iteration along a five-dimensional state vector. We use a five-dimensional grid, with the first three dimensions corresponding to $\tilde{Z}_t$, the fourth dimension corresponding to $\hat{s}_t$, and the fifth dimension corresponding to x_{t-1}.

D.1.1 Grid

In this section, we use $\tilde{Z}, \hat{s}, x$ to denote the corresponding time-t variables. We use superscripts $^-$ to denote variables in the previous period and $^+$ to denote variables in the next period. We solve numerically for f_n, b_n, and $b_n^{\$}$ as functions of the vector of state variables $\left[\tilde{Z}, \hat{s}, x^-\right]$.

Our grid is densest along the $\hat{s}$ dimension to capture important non-linearities of asset prices with respect to the surplus consumption ratio. Following Wachter (2005), we choose a grid for the surplus consumption ratio that consists of an upper segment and a lower segment and covers a wide range of values for s_t. Let $S_{grid,1}$ denote a vector of 20 equally spaced points between 0 and S_{max} with S_{max} included and $s_{grid,2}$ a vector of 30 equally spaced points between $min\left(\log\left(S_{grid,1}\right)\right)$, and -50. The grid for $\hat{s}_t = s_t - \bar{s}$ then consists of the concatenation of $s_{grid,2} - \bar{s}$ and $\log\left(S_{grid,1}\right) - \bar{s}$.

We find that bond and stock prices are close to loglinear in $\tilde{Z}$ and $\hat{x}^-$, so coarser grids are sufficient along those dimensions of the state vector. In fact, the analytic expressions for f_1, b_2, and $b_2^{\$}$ show that one-period zero-coupon consumption claims and two-period bond prices are exactly log-linear in $\tilde{Z}$ and x^-. Numerical results indicate that this property translates to longer-period claims and f_n, b_n, and $b_n^{\$}$ are still approximately linear in $\tilde{Z}$ and x^- for general n. To speed up the value function iteration, we therefore use two grid points for each dimension of $\tilde{Z}$ and for x^-.

For $\tilde{Z}$, we use an equal-spaced three-dimensional grid. Let N denote the number of grid points along each dimension and m the width of the grid as a multiple of the unconditional standard deviation of $\tilde{Z}$. For each dimension of $\tilde{Z}$, we choose a grid of N equal-spaced points with the lowest point equal to $-m \times std(\tilde{Z})$ and the highest point equal to $m \times std(\tilde{Z})$. Here, the unconditional variance-covariance matrix of $\tilde{Z}$ is determined implicitly by the equation:

$$std(\tilde{Z}) = \sqrt{\tilde{B}Var\left(\tilde{Z}\right)\tilde{B}' + diag(1,1,1)}. \tag{A195}$$

For our baseline grid, we set $N = 2$ and $m = 2$.

For x^-, we consider an equal-spaced grid with $sizexm$ points ranging from $min\left(e_1 A\tilde{Z}_t : \tilde{Z} \in grid\right)$ to $max\left(e_1 A\tilde{Z} : \tilde{Z} \in grid\right)$. This choice of grid ensures that the grid for x^- covers the entire range of output gap values implied by the grid for $\tilde{Z}$. In our baseline evaluation, we set $sizexm = 2$.

With $N = 2$ grid points along each of the three dimensions of $\tilde{Z}$, 50 gridpoints for $\hat{s}$, and $sizexm = 2$ grid points for x^-, the combined grid has a total of $2^3 \cdot 50 \cdot 2 \cdot = 800$ points.

D.1.2 Numerical integration

Following Wachter (2005), we use Gauss-Legendre quadrature to evaluate the expectations (A123), (A134), and (A139) numerically. Gauss-Legendre quadrature is orders of magnitude faster than computing expectations by simulation. As in Wachter (2005), we evaluate infinite integrals over the density of standardized consumption shocks ($\epsilon_{1,t}$) using 40 integration node points and an integration domain ranging from -8 standard deviations to $+8$ standard deviations. To conserve speed and memory, we integrate over shocks orthogonal to surplus consumption ($\epsilon_{2,t}$) using a somewhat smaller number of integration node points, 15, but again an integration domain of ± 8 standard deviations. To evaluate bond and stock prices at points that are not on the grid, we use loglinear multi-linear interpolation and extrapolation.

For completeness, we recap the key features of Gauss-Legendre integration. Let $xGL_i,\ i = 1, ..., N_{GL}$ and $wGL_i = 1, ..., N_{GL}$ denote the Gauss-Legendre nodes and weights of N_{GL}th order. Gauss-Legendre quadrature then approximates a definite integral of any smooth function f on the interval $[-1, 1]$ by $\int_{-1}^{1} f(x)\, dx \approx \sum_{i=1}^{N_{GL}} wGL_i f(xGL_i)$. By change of variable, it is immediate that we can approximate the integral of a smooth function f on an interval $[-\bar{a}, \bar{a}]$ by

$$\int_{-\bar{a}}^{\bar{a}} f(x)\, dx \approx \sum_{i=1}^{N_{GL}} \underbrace{\bar{a} \times wGL_i}_{wGL_i^{\bar{a}}} f\left(\underbrace{\bar{a} \times xGL_i}_{xGL_i^{\bar{a}}}\right). \tag{A196}$$

Here, we use $xGL_i^{\bar{a}}$ and $wGL_i^{\bar{a}}$ to denote Gauss-Legendre node points and weights scaled to the interval $[-\bar{a}, \bar{a}]$.

We implement Gauss-Legendre quadrature to take expectations over ϵ_{t+1} as follows. Let N_1 denote the number of Gauss-Legendre nodes and $\bar{a}_1$ denote the integration domain for the shock $\epsilon_{1,t}$, that is perfectly correlated with output innovations. We set $xGL_{1,i} = xGL_i^{\bar{a}_1}$ and $wGL_{1,i} = wGL_i^{\bar{a}_1}$ for $i = 1, ..., N_1$, where the weights and nodes are as defined in equation (A196). Moreover, we set

$$pGL_{1,i} = \frac{1}{\sqrt{2\pi}} exp\left(-xGL_{1,i}^2\right) wGL_{1,i} / \sum_{i=1}^{N_1} \left(\frac{1}{\sqrt{2\pi}} exp\left(-xGL_{1,i}^2\right) wGL_{1,i}\right), \tag{A197}$$

and use the scaled weights $pGL_{1,i}$ for numerical integration. The scaling of (A197) ensures that the numerical expectation of a constant is evaluated to be the same constant (or intuitively that discretized probabilities sum to one).

We then evaluate numerically the expectation of any smooth function f of $\epsilon_{1,t}$ via:

$$E\left[f\left(\epsilon_{1,t}\right)\right] = \int_{-\infty}^{\infty} \frac{1}{\sqrt{2\pi}} exp\left(-\epsilon_1^2\right) f\left(\epsilon_1\right) d\epsilon_1, \tag{A198}$$

$$\approx \int_{-\bar{a}_1}^{\bar{a}_1} \frac{1}{\sqrt{2\pi}} exp\left(-\epsilon_1^2\right) f\left(\epsilon_1\right) d\epsilon_1, \tag{A199}$$

$$\approx \sum_{i=1}^{N_1} pGL_{1,i} f\left(xGL_{1,i}\right). \tag{A200}$$

Accuracy increases with $\bar{a}_1$ and N_1. We follow Wachter (2006) in setting $N_1 = 40$ and $\bar{a}_1 = 8$.

To take expectations over $\epsilon_{2,t}$ and $\epsilon_{3,t}$, we similarly use Gauss-Legendre quadrature with integration domain $\bar{a}_2 = 8$ and number of nodes $N_2 = 15$. We set $xGL_{2,i} = xGL_i^{\bar{a}_2}$ and $wGL_{2,i} = wGL_i^{\bar{a}_2}$ for $i = 1, ..., N_2$ and define the scaled weights:

$$pGL_{2,i} = \frac{1}{\sqrt{2\pi}} exp\left(-xGL_{2,i}^2\right) wGL_{2,i} / \sum_{i=1}^{N_2} \left(\frac{1}{\sqrt{2\pi}} exp\left(-xGL_{2,i}^2\right) wGL_{2,i}\right), \tag{A201}$$

The weights and nodes for $\epsilon_{3,t}$ are identical to those of $\epsilon_{2,t}$.

Since $\epsilon_{1,t}$, $\epsilon_{2,t}$, and $\epsilon_{3,t}$ are independent, we can evaluate the expectation of any smooth function $f\left(\epsilon_{1,t}, \epsilon_{2,t}, \epsilon_{2,t}\right)$ as

$$Ef\left(\epsilon_{1,t}, \epsilon_{2,t}, \epsilon_{3,t}\right) = \int_{-\infty}^{\infty} \frac{1}{\sqrt{2\pi}} exp\left(-\epsilon_1^2\right) \int_{-\infty}^{\infty} \frac{1}{\sqrt{2\pi}} exp\left(-\epsilon_2^2\right) \int_{-\infty}^{\infty} \frac{1}{\sqrt{2\pi}} exp\left(-\epsilon_3^2\right) f\left(\epsilon_1, \epsilon_2, \epsilon_3\right) d\epsilon_1 d\epsilon_2 d\epsilon_3$$

$$\approx \sum_{i=1}^{N_1} pGL_{1,i} \left[\sum_{j=1}^{N_2} pGL_{2,j} \left[\sum_{k=1}^{N_3} pGL_{3,k} f\left(xGL_{1,i}, xGL_{2,j}, xGL_{3,k}\right)\right]\right]. \tag{A202}$$

D.1.3 Recursive step

Let a superscript ^{num} denote the numerical counterparts to the analytic functions f_n, b_n, $b_n^{\$}$. We start by initializing $f_1^{num}\left(\tilde{Z}, \hat{s}, x^-\right)$, $b_2^{num}\left(\tilde{Z}, \hat{s}, x^-\right)$, and $b_2^{\$,num}\left(\tilde{Z}, \hat{s}, x^-\right)$ at each grid point according to the analytic expressions (A121), (A131) and (A133).

Next, we apply the recursive expressions (A123), (A134), and (A139) along the grid. Having computed f_{n-1}^{num} along the entire grid, we evaluate $f_n^{num}\left(\tilde{Z}, \hat{s}, x^-\right)$ at a grid point

$\left(\tilde{Z}, \hat{s}, x^{-}\right)$ as follows. We compute the expectation (A123) numerically as:

$$
\begin{aligned}
f_n^{num}(\tilde{Z}, \hat{s}, x^{-}) \;=\; & \log \left[\sum_{i=1}^{N_1} pGL_{1,i} \left[\sum_{j=1}^{N_2} pGL_{2,j} \left[\sum_{k=1}^{N_3} pGL_{3,k} \cdot \exp \Big(g + e_1 [B - \phi I] A^{-1} \tilde{Z} \right.\right.\right. \\
& - \bar{r} - (1 - \rho^a)(e_3 - e_2 B) A^{-1} \tilde{Z} - \frac{\gamma}{2}(1 - \theta_0)(1 - 2\hat{s}) \\
& - (\gamma(1 + \lambda(\hat{s})) - 1)\sigma_c \times xGL_{1,i} \\
& \left.\left.\left. + f_{n-1}^{num} \left(\tilde{B}\tilde{Z} + \begin{bmatrix} xGL_{1,i} \\ xGL_{2,j} \\ xGL_{3,k} \end{bmatrix}, \theta_0 \hat{s} + \theta_1 x + \theta_2 x^{-} + \lambda(\hat{s})\, xGL_{1,i}, x \right) \Big) \right]\right]\right],
\end{aligned}
\tag{A203}
$$

where we evaluate x as a function of the state vector as

$$
x \;=\; e_1 A^{-1} \tilde{Z}. \tag{A204}
$$

To compute the right-hand-side of (A203), we need to evaluate f_{n-1}^{num} at points that are not on our grid. We interpolate f_{n-1}^{num} linearly (and hence F_{n-1}^{num} log-linearly). When the argument is outside the range of the grid, we extrapolate f_{n-1}^{num} linearly. It is clear from (A121) that linear inter- and extrapolation gives a good approximation of f_1. In fact, we can see that f_1 is exactly linear in $\tilde{Z}$, independent of x^{-}, and that it depends on $\lambda(\hat{s}) = \lambda_0\sqrt{1-2\hat{s}}$. We accommodate the fact that f_1 is not linear in $\hat{s}$ by choosing a much denser grid along the $\hat{s}$ dimension. We do not have analytic expressions for $f_n, n > 1$ (after all, that's why we need a numerical solution), but numerical solutions indicate that linear inter- and extrapolation gives good approximations for f_n with the chosen grid.

In terms of coding (A203), we face a trade-off between speed and readability of the code. We pre-allocate matrices outside loops and we code linear interpolation by hand (rather than using a pre-written interpolation routine) to conserve speed and memory. We also inline the linear interpolation steps (i.e. write them directly into the main function rather than calling a separate interpolation function). This speeds up the code substantially, while reducing its readability.

There are different methods to interpolate multidimensional functions. Specifically, we use multi-linear interpolation, corresponding to interpolating along each dimension one at a time. In order to enhance computational speed we do not rely on a pre-programmed interpolation routine, instead coding our own minimal interpolation routine. It is well-known that the result of multi-linear (or in the two-dimensional case bi-linear) interpolation does not depend on in which order one interpolates the different arguments. We find it convenient to interpolate $f_{n-1}^{num}\left(\tilde{Z}, \hat{s}, x^{-}\right)$ first along the x^{-} dimension, then along $\hat{s}$, then along $\tilde{Z}_1$, and finally along the $\tilde{Z}_2$ and $\tilde{Z}_3$ dimensions.

Finally, we evaluate the price-consumption ratio for the aggregate consumption stream by approximating it as the sum of the first 300 zero-coupon consumption claims:

$$
F^{num}\left(\tilde{Z}_t, \hat{s}_t, x_{t-1}\right) \;=\; \sum_{n=1}^{300} exp\left(f_n^{num}(\tilde{Z}_t, \hat{s}_t, x_{t-1})\right). \tag{A205}
$$

We iterate $b_n^{num}\left(\tilde{Z},\hat{s},x^-\right)$ and $b_n^{\$,num}\left(\tilde{Z},\hat{s},x^-\right)$ similarly according to:

$$\begin{aligned} b_n^{num}(\tilde{Z}_t,\hat{s}_t,x_{t-1}) = & \log\left[\sum_{i=1}^{N_1} pGL_{1,i}\left[\sum_{j=1}^{N_2} pGL_{2,j}\left[\sum_{k=1}^{N_3} pGL_{3,k}\right.\right.\right. \\ & \cdot\exp\left(-\bar{r}-(e_3-e_2B)A^{-1}\tilde{Z}-\frac{\gamma}{2}(1-\theta_0)(1-2\hat{s})\right. \\ & -\gamma(1+\lambda(\hat{s}))\sigma_c\times xGL_{1,i} \\ & \left.\left.\left.\left.+b_{n-1}^{num}\left(\tilde{B}\tilde{Z}+\begin{bmatrix} xGL_{1,i}\\ xGL_{2,j}\\ xGL_{3,k}\end{bmatrix},\theta_0\hat{s}+\theta_1x+\theta_2x^-+\lambda(\hat{s})\,xGL_{1,i},x\right)\right]\right]\right]\right], \end{aligned} \tag{A206}$$

and

$$\begin{aligned} b_n^{\$,num}(\tilde{Z}_t,\hat{s}_t,x_{t-1}) = & \left[\sum_{i=1}^{N_1} pGL_{1,i}\left[\sum_{j=1}^{N_2} pGL_{2,j}\left[\sum_{k=1}^{N_3} pGL_{3,k}\right.\right.\right. \qquad \text{(A207)} \\ & \cdot\exp\left(-\bar{r}-e_3A^{-1}\tilde{Z}-\frac{\gamma}{2}(1-\theta_0)(1-2\hat{s})\right. \\ & -\left(\gamma(1+\lambda(\hat{s}))\sigma_c+vpi_1+n\cdot vec^*e_1'\right)\times xGL_{1,i} \\ & -\left(vpi_2+n\cdot vec^*e_2'\right)xGL_{2,j}+\frac{n^2}{2}\left(\sigma^\perp\right)^2 \\ & \left.\left.\left.\left.+b_{n-1}^{\$,num}\left(\tilde{B}\tilde{Z}+\begin{bmatrix} xGL_{1,i}\\ xGL_{2,j}\\ xGL_{3,k}\end{bmatrix},\theta_0\hat{s}+\theta_1x+\theta_2x^-+\lambda(\hat{s})\,xGL_{1,i},x\right)\right]\right]\right]\right], \end{aligned} \tag{A208}$$

We again use multi-linear interpolation and extrapolation to evaluate $b_{n-1}^{\$,num}$ and b_{n-1}^{num} at points that are not on the grid. We similarly implement the recursions (A164), (A166), and (A173) numerically to obtain risk-neutral bond and consumption claim valuations $B_n^{rn,num}$, $B_n^{rn,\$,num}$, $G^{rn,num}$.

D.2 Simulating the Model

We simulate a draw of length T. Results in Tables 2 and Table 4 use $T = 10000$ and discard the first 100 simulation periods to ensure that the system has reached the stochastic steady-state. We report model moments averaged across 2 independent simulations.

We use superscript *sim* to denote simulated quantities. We use the MATLAB function mvnrnd to obtain independent draws $v_t^{sim} \sim N(0,\Sigma_v)$ for $t = 1,2,...,T$. We then obtain the rotated shock according to $\epsilon_t^{sim} = Av_t^{sim}$ and $v_t^{LT,sim} = e_4v_t^{sim}$. We generate draws for $\tilde{Z}_t^{sim}, t = 1,...,T$ by setting $\tilde{Z}_1^{sim} = 0$ and then updating according to (A94). We obtain the simulated non-rotated state vector for $t = 1,2,...,T$ through the relation $Y_t^{sim} = A^{-1}\tilde{Z}_t^{sim}$. We generate draws for the surplus consumption ratio by setting $\hat{s}_1^{sim} = 0$ and $x_0^{sim} = 0$ and then updating according to (A103). We generate the simulated random walk component of inflation $v_t^*, t = 1,2,...,T$ by starting from $v_1^{*sim} = 0$ and updating it according to equation (22) in the main paper. We initialize simulated log consumption at $c_1^{sim} = 0$ and update it using (26). We then drop the first 100 simulation periods to allow the system to converge to the stochastic steady-state.

Having generated draws for the five state variables $\tilde{Z}^{sim}$, $\hat{s}^{sim}$, and x_{t-1}^{sim}, we obtain the simulated consumption-claim price-dividend ratio as $(P^c/C)_t^{sim} = F^{num}\left(\tilde{Z}_t^{sim}, \hat{s}_t^{sim}, x_{t-1}^{sim}\right)$, n-period real bond prices as
$P_{n,t}^{sim} = B_n^{num}\left(\tilde{Z}_t^{sim}, \hat{s}_t^{sim}, x_{t-1}^{sim}\right)$, and
$B_{n,t}^{\$,sim} = B_n^{\$,num}\left(\tilde{Z}_t^{sim}, \hat{s}_t^{sim}, x_{t-1}^{sim}\right)$. We obtain the corresponding risk-neutral valuation ratios by plugging into the risk-neutral asset pricing solutions:
$(P^c/C)_t^{rn,sim} = F^{rn,num}\left(\tilde{Z}_t^{sim}, \hat{s}_t^{sim}, x_{t-1}^{sim}\right)$,
$P_{n,t}^{rn,sim} = B_n^{rn,num}\left(\tilde{Z}_t^{sim}, \hat{s}_t^{sim}, x_{t-1}^{sim}\right)$, and
$B_{n,t}^{rn,\$,sim} = B_n^{rn,\$,num}\left(\tilde{Z}_t^{sim}, \hat{s}_t^{sim}, x_{t-1}^{sim}\right)$. We obtain nominal bond prices $P_{n,t}^{\$,sim}$ by combining $B_{n,t}^{\$,sim}$ and v_t^{*sim} according to (A125). We similarly obtain risk-neutral nominal bond prices $P_{n,t}^{rn,\$,sim}$ by combining $B_{n,t}^{rn,\$,sim}$ and v_t^{*sim} according to (A125).

To deal with the fact that $\tilde{Z}_t^{sim}$, $\hat{s}_t^{sim}$, x_{t-1}^{sim} are not usually on grid points we adopt a similar linear interpolation strategy as in the numerical evaluation of the asset pricing recursions described in Section D.1.3. We interpolate F^{num}, B_n^{num}, and $B_n^{\$,num}$ log-linearly. We simplify the interpolation strategy slightly compared to Section D.1.3. We use the MATLAB function griddedInterpolant, sacrificing some computational speed for simpler code. Even though rare events (and especially extremely negative realizations for $\hat{s}$) matter for the value function iteration in Section D.1.3, low-probability events have very little impact on the properties of simulated asset prices taking as given F^{num}, B^{num}, and $B^{\$,num}$. We therefore simplify the log-linear interpolation by truncating $\tilde{Z}_t^{sim}$, $\hat{s}_t^{sim}$, and x_{t-1}^{sim} at the maximum and minimum values covered by the grid.

Having generated $\left(\frac{P^c}{C}\right)_t^{sim}, t = 1, ..., T$, we compute log returns on the consumption claim $r_{t+1}^{c,sim}$ according to (A141). We obtain simulated price-dividend ratios for levered stocks by plugging into (A148). Finally, we obtain log bond yields and stock and bond excess returns as described in Section C.5.3. Risk-neutral bond and stock returns are computed by substituting $\left(\frac{P^c}{C}\right)^{rn,sim}$, $P_{n,t}^{rn,\$,sim}$, and $P_{n,t}^{rn,sim}$ into the same relations.

We simulate pre-FOMC asset prices as follows. We use the MATLAB function mvnrnd to generate independent draws for the FOMC shock
$v_t^{FOMC,sim} \sim N\left(0, diag\left(\left[0, 0, \left(\sigma_{ST}^{FOMC}\right)^2, \left(\sigma_{LT}^{FOMC}\right)^2\right]\right)\right)$, where $t = 1, ..., T$. Having drawn the FOMC shock $v_t^{FOMC,sim}$ we obtain the simulated pre-FOMC component of the overall quarterly simulated shock as

$$v_t^{pre,sim} = v_t^{sim} - v_t^{FOMC,sim}, \tag{A209}$$
$$\epsilon_t^{pre,sim} = A v_t^{pre,sim}. \tag{A210}$$

We then use the simulated values for $\tilde{Z}_{t-1}^{sim}$, Y_{t-1}^{sim}, c_{t-1}^{sim}, $\hat{s}_{t-1}^{sim}$, v_{t-1}^{*} and $\epsilon_t^{pre,sim}$ to compute the simulated pre-FOMC state vector according to equations (A178) through (A182). We then obtain pre-FOMC asset prices by substituting the simulated pre-FOMC state vector into equations (A183) through (A182). Simulated yield changes around FOMC news are then computed according to equations (A189) and (A192) and simulated FOMC stock returns are obtained according to equation (A194).

D.3 Parameter units

This subsection details the relation between parameter values in empirical (reported in the paper) and natural units (used for solving the code). We solve the model in natural units. However, it is most natural to report empirical moments and summary statistics in empirical units for interpretability.

For comparability with empirical moments, Table 1 reports model parameters in units that correspond to the output gap in annualized percent, and inflation and interest rates in annualized percent. As in Campbell, Pflueger, and Viceira (2020), we report the discount rate and the persistence of surplus consumption in annualized units. Concretely, Table 1 reports the following scaled parameters:

$$400 \times g, \tag{A211}$$
$$400 \times \bar{r}, \tag{A212}$$
$$\theta_0^4, \tag{A213}$$
$$\beta^4, \tag{A214}$$
$$4 \times \gamma^x \tag{A215}$$
$$100 \times \sigma_x, \tag{A216}$$
$$400 \times \sigma_\pi, \tag{A217}$$
$$400 \times \sigma_{ST}, \tag{A218}$$
$$400 \times \sigma_{LT}, \tag{A219}$$
$$\frac{1}{4} \times \psi, \tag{A220}$$
$$4 \times \kappa \tag{A221}$$

All other parameters reported in Table 1 do not need to be scaled.

E Details: Simulated Method of Moments

E.1 Reduced-Form Impulse Responses

This section describes how we estimate the macroeconomic impulse responses reported in Figure 2. We follow the procedure described below for both actual and simulated data, with the simulated data length matching the length of the empirical sample. Model impulse responses in Figures 2 are averaged over 100 simulations. In this section, we use subscripts IRF if variable names would otherwise be similar to different variables elsewhere in the paper.

To account for the unit root in inflation in the model, we estimate a vector error correction model of the form

$$Y_{IRF,t} = \Pi Y_{IRF,t-1} + \varepsilon_t \tag{A222}$$

where we define the vector for the VECM as:

$$Y_{IRF,t} = [x_{t-1}, \pi_t - \pi_{t-1}, i_t - \pi_t]. \tag{A223}$$

This definition of the VAR(1) vector guarantees that each of the variables is stationary when the data is simulated from our model since the unit root affects the short-term interest rate i_t only through its effect on inflation π_t.

The shocks ε_t are not orthogonal and we denote their estimated variance-covariance matrix by Σ_ε. Next, we rotate the innovations to be orthogonal. This means that we need to re-write (A222) in the form:

$$R^{-1} Y_{IRF,t} = \Pi_R Y_{IRF,t-1} + \eta_t \tag{A224}$$

where η_t is a vector of uncorrelated shocks, R is an invertible matrix, and $\Pi_R = R^{-1}\Pi$. We write the variance-covariance matrix of η_t as:

$$\Sigma_\eta = \mathbb{E}\eta_t'\eta_t = \begin{bmatrix} \sigma(\eta_1)^2 & 0 & 0 \\ 0 & \sigma(\eta_2)^2 & 0 \\ 0 & 0 & \sigma(\eta_3)^2 \end{bmatrix} \tag{A225}$$

We pick R^{-1} to be lower-diagonal with ones along the diagonal. Having estimated Π and Σ_ε we obtain R, Π_R, and Σ_η using Cholesky factorization.

We then construct impulse responses. We start with a unit standard deviation orthogonalized shock to output gap:

$$\eta_1 = [\sigma(\eta_1), 0, 0] \tag{A226}$$

which is equivalent to

$$\varepsilon_1 = R[\sigma(\eta_1), 0, 0]. \tag{A227}$$

The n-th response to a one standard deviation shock to the output gap then is computed as:

$$\Pi^{n-1}\varepsilon_1 = \Pi^{n-1} R[\sigma(\eta_1), 0, 0]. \tag{A228}$$

We can similarly compute the responses for the change in inflation $\pi_t - \pi_{t-1}$ and the difference between the nominal interest rate and inflation $i_t - \pi_t$. In order to then obtain the corresponding responses of inflation, we cumulate the responses of $\pi_t - \pi_{t-1}$ and finally add the response of inflation to that of $i_t - \pi_t$ to obtain the response of the short-term nominal interest rate.

E.2 Confidence intervals and objective function

We use a bootstrap method to compute confidence intervals for the empirical impulse responses shown in Figure 2 and for the variances of the impulse responses used in the SMM estimation. Let Π and Σ_ε denote the coefficient matrix and the variance-covariance matrix of shocks from estimating (A222) on actual data. We then generate bootstrapped data by simulating $Y^{boot}_{IRF,t}$ of identical sample length as the true data according to

$$Y^{boot}_{IRF,t} = \Pi Y^{boot}_{IRF,t-1} + \varepsilon^{boot}_t, \tag{A229}$$

where ε_t^{boot} are drawn as iid normal with mean zero and variance-covariance Σ_ε. On the bootstrapped data, we then apply the methodology for IRFs described in Section E.1. That is, we re-estimate (A222) on the bootstrapped data and use the resulting estimates to construct bootstrapped impulse response functions. We generate 1000 independent bootstrap samples. Figure 2 shows confidence intervals, such that 95% of the time the bootstrapped impulse responses are within the interval.

For our objective function, we define the empirical target moments as follows. $\hat{\Psi}$ is $[15 \times 1]$. It includes $15 = 6 \cdot 3 - 3$ impulse responses. We have 15 impulse response moments, because we have nine impulse responses at zero (shock period), one, two, four, eight, and twelve quarters each. However, three of the shock period impulse responses are zero by our choice of orthogonalization and we exclude them from the objective function.

Let $\hat{V}$ denote the bootstrapped variance-covariance matrix of $\hat{\Psi}^{boot} - \hat{\Psi}$. We then define the weighting matrix $\hat{W}$ for the SMM objective function as the diagonal matrix with the inverse variances for the 15 impulse response moments along the diagonal:

$$\hat{W} \quad = \quad diag(inv(\hat{V}_{1,1}), inv(\hat{V}_{2,2}), ..., inv(\hat{V}_{51,51})). \tag{A230}$$

The SMM objective function is then given by equation (39) in the main text.

E.3 Grid search

We minimize the objective function $J(\sigma)$ using a two-step grid search. To reduce the need to compute (computationally expensive) asset prices along the grid, we separate the parameters into $[\sigma_x, \sigma_\pi, \sigma_{ST}]$ and σ_{LT}. The first step of the grid search finds the parameter values for $[\sigma_x, \sigma_\pi, \sigma_{ST}]$ that minimize the objective function while holding the volatility of the long-term monetary policy shock constant at $\sigma_{LT} = 0.25$, which we have chosen to match roughly the volatility of changes in 10-on-10-year breakeven, which equals 0.26% in our empirical sample. In this first grid search step, we solve and simulate macroeconomic dynamics and reduced-form impulse responses (but not asset prices) over a grid for the first three volatility parameters. We choose an equally-spaced grid with 20 points between 0.01 and 1 for each of σ_x, σ_π, and σ_{ST}, so we evaluate the macroeconomic dynamics at a total of $20^3 = 8000$ gridpoints in this step. We discard parameter values in this step, where asset prices do not exist.

In a second step, we find the volatility of the long-term monetary policy shock σ_{LT} by minimizing the distance between the volatility of changes in 10-on-10 year breakeven in the model and in the data, while holding all other model parameters constant. This second step requires solving for asset prices at each grid point, and is hence substantially slower than the first step. We evaluate the model volatility of changes in 10-on-10-year breakeven inflation on an equally-spaced grid for σ_{LT} with 20 points between 0.01 and 1. Because it takes about 2 minutes to solve for macroeconomic dynamics and asset prices, this second step of the grid search takes about $2 \times 20 = 40$ minutes. We again discard parameter vectors where asset prices do not exist.

F Additional Model Results

F.1 Switching off model components

Table A1 shows that the model results described in Table 4 are robust to switching off individual model components. For instance, reducing the equilibrium volatility of Phillips curve, short-term monetary policy, or long-term monetary policy shocks leaves the relationship of stock returns and monetary policy surprises on FOMC dates unchanged. For the counterfactual exercises in columns (5) and (6) of Table A1 monetary policy shocks on FOMC dates are still non-zero, but they are unanticipated and out-of-equilibrium because the equilibrium volatility of monetary policy shocks set to zero.

The model results for high-frequency stocks and bonds around FOMC announcements are robust to switching off the link between expected growth and the short-term real rate by setting $\rho_a = 0$. Table A1, column (1) shows that the model regression coefficients are actually somewhat larger when we switch off this link, and that time-varying risk premia continue to represent about 50% of the overall stock response to monetary policy news. With $\rho^a = 0$, a surprise increase in the short-term monetary policy rate is not accompanied by higher growth expectations, so stocks fall even more than in our baseline calibration. The link between the short-term real rate and expected growth ($\rho^a > 0$) in our baseline calibration therefore helps, because it ensures that the stock return response to monetary policy shocks is not too large compared to the data, as in Nakamura and Steinsson (2018).

Switching off the habit shock in column (3) also increases the model slope coefficients around FOMC announcements, and continues to imply a substantial risk premium response, as in the baseline calibration. Intuitively, in the absence of independent habit shocks the consumption claim is conditionally perfectly correlated with surplus consumption, so stocks are even riskier for investors.

Table A1: Model Decomposition

	(1) Baseline	(2) $\rho^a = 0$	(3) $\sigma_x = 0$	(4) $\sigma_\pi = 0$	(5) $\sigma_{ST} = 0$	(6) $\sigma_{LT} = 0$
Panel A: Overall monetary policy shocks effect						
Slope(S&P 500 Return, Fed Funds)	-5.27	-11.38	-15.43	-5.15	-4.96	-5.20
Slope(S&P 500 Return, 10Y Breakeven)	5.89	11.54	17.00	5.74	5.54	5.81
Panel B: Monetary policy shocks effect on risk premia						
Slope(S&P 500 Risk Premium, Fed Funds)	-2.54	-7.71	-14.16	-2.49	-2.21	-2.46
Slope(S&P 500 Risk Premium, 10Y Breakeven)	2.7	7.57	15.34	2.64	2.35	2.63
Panel C: Bond Betas						
Real Bond-Stock Beta	0.03	0.07	0.17	0.02	-0.02	0.01
Breakeven-Stock Beta	-0.13	-0.16	-0.22	-0.13	-0.11	-0.04

Note: This table compares asset pricing moments while switching off individual model components. The real and breakeven stock betas are computed as in Table 2, and the asset price reactions around monetary policy dates are as in Table 4. Column (1) of Panel A repeats the model regression of Table 4, column (2). The remaining columns of Panel A report the corresponding model regression coefficients while switching off individual model components. Panel B reports regression estimates corresponding to Table 4, column (4), where the dependent variable is the risk premium component of equity returns. For all panels, column (1) repeats the baseline model results. Column (2) switches off predictable technology growth. Column (3) sets the demand shock to zero. Column (4) sets the Phillips curve shock to zero. Column (5) sets the short-term monetary policy shock to zero. Column (6) sets the long-term monetary policy shock to zero. For the counterfactual exercises in columns (5) and (6) of Table A1 monetary policy shocks on FOMC dates are still non-zero, but they are unanticipated and out-of-equilibrium because the equilibrium volatility of monetary policy shocks set to zero. All other parameters are held constant at the values listed in Table 1.

F.2 Model Real Bond Yields around FOMC Announcements

In this Appendix Section, we show that our model matches the comovement between the short-term nominal interest rate and long-term real bond yields around FOMC dates, which Nakamura and Steinsson (2018) and Hanson and Stein (2015) have documented.

Table A2: Data and Model Real Bond Yields around FOMC Announcements

	(1) Data	(2) Model	(3) Model ($\rho^a = 0$)
Slope(5Y Real Yield, Fed Funds)	0.42* (0.22)	0.36	0.32
Risk Neutral		0.35	0.29
Slope(10Y Real Yield, Fed Funds)	0.28* (0.16)	0.17	0.18
Risk Neutral		0.17	0.15

Note: This table compares the comovement of long-term real bond yields and short-term nominal interest rates around monetary policy announcements in the model and in the data. The table reports coefficient estimates from regressions of the form $\Delta^{FOMC} y_{n,t} = b_0 + b_1 \Delta^{FOMC} i_t + \varepsilon_t$, where $\Delta^{FOMC} y_{n,t}$ is either the change in the 10-year or 5-year real bond yield from the day before the FOMC announcement to the day after. We use zero-coupon TIPS yields from Gürkaynak, Sack, and Wright (2010). The surprise in the Federal Funds rate and the sample are as in Table 4. Model asset price changes around FOMC announcements are also as described in Table 4. Risk neutral rows show the slope coefficients when model long-term real bond yields are computed from the stochastic discount factor of a risk neutral investor taking macroeconomic dynamics as given.

Table A2 shows that our model matches the empirical relationship between long-term real yields and short-term nominal yields on FOMC days:

$$\Delta^{FOMC} y_{n,t} \quad = \quad b_0 + b_1 \Delta^{FOMC} i_t + \varepsilon_t, \tag{A231}$$

where $\Delta^{FOMC} y_{n,t}$ is the change in either the 10-year or the 5-year real bond yield and $\Delta^{FOMC} i_t$ is the change in the Federal Funds rate. Table A2, column (1) shows that long-term real bond (TIPS) yields indeed move with surprises in short-term interest rates in our sample, consistent with prior empirical results. In the data, a 25 bps surprise increase in the short-term nominal interest rate tends to be accompanied by a substantial 11 bps increase in the 5-year TIPS yield and a 7 bps increase in the 10-year TIPS yield.

Column (2) shows that the model replicates the positive empirical relationship between long-term real bond yields and short-term nominal yields on FOMC dates. In the model, a 25 bps point increase in short-term nominal yield is associated with a 9 bps increase in the 5-year real bond yield, and a 4 bps increase in the 10-year real bond yield, similarly to the data. Both of these coefficients are economically meaningful and within two standard deviations of the empirical estimates, though smaller than in the data.

One might expect that setting $\rho^a > 0$ (as in our baseline calibration) should lead to higher model regression coefficients in Table A2. The standard intuition in Nakamura and Steinsson (2018) is that when monetary policy is perceived to follow the natural rate implied by expected growth, a surprise increase in the policy rate leads investors to update about expected growth going forward, thereby raising long-term real bond yields. Consistent with this intuition, column (3) shows that switching off the link between productivity growth and the real yields ($\rho^a = 0$) indeed weakens the link between short-term nominal and 5-year real bond yields. For the 10-year bond yields, setting $\rho^a = 0$ does not reduce the model slope coefficient of 10-year real bond yields onto the short-term policy rate around monetary policy announcements.

Looking at the slope coefficients for risk-neutral real bond yields provides an answer to this puzzling result. We compute risk-neutral real bond yields according to the expectations hypothesis, so they contain no risk premia. As expected, switching off the real rate - growth link ($\rho^a = 0$) weakens the slope coefficients of model risk-neutral real bond yields onto short-term policy rate surprises for both the 5-year and the 10-year real bond maturities. The role for risk premia in our model arises because whether real bond prices benefit from flight-to-safety is endogenous to the macroeconomic regime (including ρ^a). Table A1, Panel C shows that when investors do not learn about growth ($\rho^a = 0$) the real bond beta is positive, so real bonds are risky. Conversely, when investors learn about expected growth from interest rates ($\rho^a > 0$), the real bond beta is closer to zero and real bonds have greater hedging benefits for investors. Intuitively, when investors associate high interest rates with growth, negative real bond returns are associated with good macroeconomic news, driving down real bond betas and improving their risk profile for the representative agent. In turn, investors prefer to hold real bonds when investor risk aversion rises after a contractionary short-term monetary policy shock, dampening the increase in long-term real bond yields. This countervailing risk premium channel suggests that larger or more persistent changes in growth expectations may be required to explain any given empirical link between long-term real bond yields and short-term policy rates on FOMC dates.

Overall, we find that our model can replicate the empirical relationship between innovations in short-term nominal and long-term real bond yields around FOMC announcements, and endogenous flight-to-safety means that even greater variation in expected growth may be justified to explain the data.

F.3 Robustness Model FOMC Results

Table 4 and Figure 5 report the slope coefficients b_1 and b_2 from running the following regression on simulated model data

$$r_t^{\delta,FOMC} = b_0 + b_1 \Delta i_t^{FOMC} + b_2 \Delta breakeven_{n,t} + \varepsilon_t. \tag{A232}$$

We pick standard deviations for the ST and LT monetary policy shocks on FOMC days to match the empirical standard deviations of our respective proxies for those shocks: 4.3 bps and 3.3 bps. To make sure that our results on the relationship of monetary policy shocks and equity returns are not driven by the choice of those exact values, in Figure A1 we plot the estimates for b_1 and b_2 while varying $\sigma_{ST}^{FOMC}/\sigma_{LT}^{FOMC}$.

Figure A1: Model High-Frequency Regression Coefficients against Volatility of FOMC ST Monetary Policy Shock

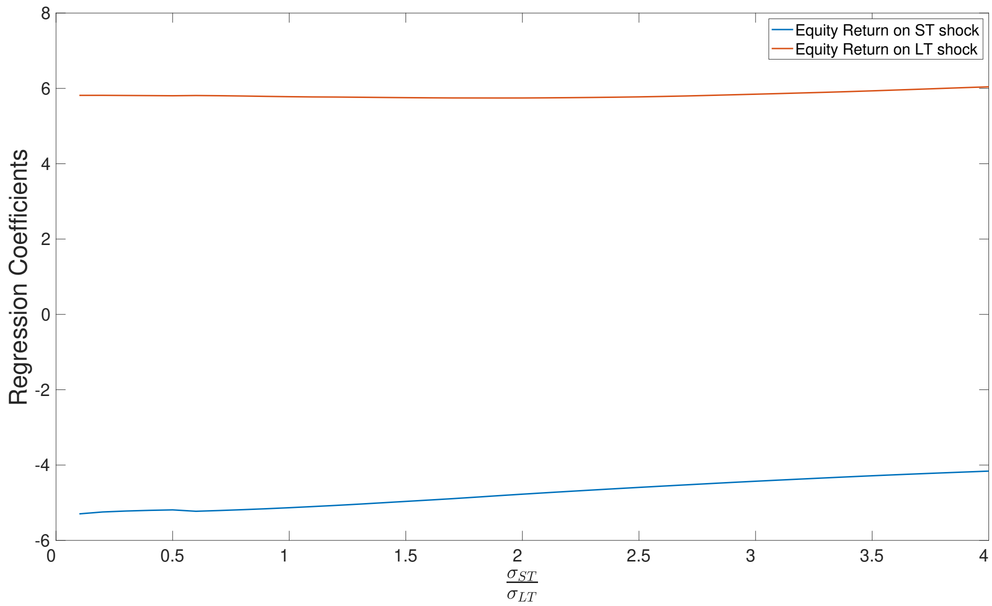

Note: This figure shows regression coefficients b_1 and b_2 from the model regression (A232), also shown in column (2) in Table 4 in the main paper. Each dot in the figure corresponds to a model simulation with a different value for the volatility of short-term monetary policy shocks realized on FOMC dates σ_{ST}^{FOMC}. We hold the volatility of the long-term monetary policy shock realized on FOMC dates constant at its baseline value of $\sigma_{LC}^{FOMC} = 3.3$ bps. We plot the model regression coefficients b_1 and b_2 on the y-axis against the ratio of the short-term to long-term monetary policy shocks realized on FOMC dates $\frac{\sigma_{ST}^{FOMC}}{\sigma_{FOMC}^{LT}}$ on the x-axis.

G Additional Empirical Results

Our model predicts that stock returns should be more sensitive to monetary policy news following a sequence of bad shocks, such as during a crisis. To verify that this prediction is in line with the data, in this section we tabulate the properties of stock returns in narrow windows around FOMC announcements during the depth of the financial crisis of 2008-09 (defined as October 2008 through December 2009).

In terms of summary statistics, we have 10 observations during this crisis period. The standard deviation of 1-hour stock returns is 1.04%, the standard deviation of Fed Funds rate innovations over the same time interval is 4.3 bps, and the standard deviation of breakeven changes on FOMC days is 3.4 bps. For comparison, our full sample has 146 FOMC date observations, with a standard deviation of 1-hour stock returns of 0.67% and virtually identical standard deviations for Federal Funds rate and breakeven surprises. During the crisis period, stock returns around FOMC announcements were hence about 50% more volatile, even though the proxies for monetary policy news were about equally as volatile as during the full sample.

Table A3 estimates the slope coefficients of stock returns onto Federal Funds rate surprises and breakeven changes around FOMC announcements for the crisis period, analogously to Table 3 columns (1) through (3). As predicted by theory, the slope coefficients are larger in magnitude during this period, which was characterized by a steep recession and high risk premia. Unfortunately, due to the small sample size, the standard errors are substantially larger than before, and we lose statistical significance.

Table A3: Empirical Equity Returns and Monetary Policy Surprises during 2008-09 Financial Crisis

	Dependent variable:		
	S&P 500 Return		
	(1)	(2)	(3)
FF Shock	−6.66		−4.23
	(4.85)		(6.46)
10Y Breakeven		10.26	8.22
		(8.81)	(10.38)
Constant	0.33	0.07	0.07
	(0.38)	(0.25)	(0.28)
Observations	10	10	10
R^2	0.08	0.09	0.14

Note: Regressions are analogous to Table 3 columns (1) through (3), except that this table uses the crisis subsample (October 2008 through December 2009).

APPENDIX REFERENCES

Campbell, John Y, and John H Cochrane, 1999, By force of habit, *Journal of Political Economy* 107, 205-251.

Campbell, John Y, Carolin Pflueger, and Luis M Viceira, 2020, Macroeconomic drivers of bond and equity risks, *Journal of Political Economy* 128, 3148–3185.

Cogley, Timothy, and Argia M. Sbordone, 2008, The time-varying volatility of macroeconomic fluctuations, *American Economic Review* 98, 2101–2126.

Greenwood, Jeremy, Zvi Hercowitz, and Gregory W Huffman, 1988, Investment, capacity utilization, and the real business cycle, *American Economic Review* pp. 402–417.

Hanson, Samuel G, and Jeremy C Stein, 2015, Monetary policy and long-term real rates, *Journal of Financial Economics* 115, 429–448.

Nakamura, Emi, and Jón Steinsson, 2018, High-frequency identification of monetary nonneutrality: the information effect, *Quarterly Journal of Economics* 133, 1283–1330.

Smets, Frank, and Rafael Wouters, 2007, Shocks and frictions in us business cycles: A Bayesian DSGE approach, *American Economic Review* pp. 586–606.

Wachter, Jessica A., 2005, Solving models with external habit, *Finance Research Letters* 2, 210–226.

Walsh, Carl E, 2017, *Monetary theory and policy* (MIT press).

Woodford, Michael, 2003, *Interest and Prices* (Princeton University Press)